Simulating the Effect of Aerobic Biodegradation on Soil Vapor Intrusion into Buildings

Evaluation of Low Strength Sources Associated with Dissolved Gasoline Plumes

API PUBLICATION 4775
APRIL 2009

Simulating the Effect of Aerobic Biodegradation on Soil Vapor Intrusion into Buildings

Evaluation of Low Strength Sources Associated with Dissolved Gasoline Plumes

Regulatory and Scientific Affairs Department

API PUBLICATION 4775
APRIL 2009

PREPARED UNDER CONTRACT BY:

LILIAN D. V. ABREU, ROBERT ETTINGER, AND TODD MCALARY
GEOSYNTEC CONSULTANTS, INC.

Special Notes

API publications necessarily address problems of a general nature. With respect to particular circumstances, local, state, and federal laws and regulations should be reviewed.

Neither API nor any of API's employees, subcontractors, consultants, committees, or other assignees make any warranty or representation, either express or implied, with respect to the accuracy, completeness, or usefulness of the information contained herein, or assume any liability or responsibility for any use, or the results of such use, of any information or process disclosed in this publication. Neither API nor any of API's employees, subcontractors, consultants, or other assignees represent that use of this publication would not infringe upon privately owned rights.

API publications may be used by anyone desiring to do so. Every effort has been made by the Institute to assure the accuracy and reliability of the data contained in them; however, the Institute makes no representation, warranty, or guarantee in connection with this publication and hereby expressly disclaims any liability or responsibility for loss or damage resulting from its use or for the violation of any authorities having jurisdiction with which this publication may conflict.

API publications are published to facilitate the broad availability of proven, sound engineering and operating practices. These publications are not intended to obviate the need for applying sound engineering judgment regarding when and where these publications should be utilized. The formulation and publication of API publications is not intended in any way to inhibit anyone from using any other practices.

Any manufacturer marking equipment or materials in conformance with the marking requirements of an API standard is solely responsible for complying with all the applicable requirements of that standard. API does not represent, warrant, or guarantee that such products do in fact conform to the applicable API standard.

Foreword

Nothing contained in any API publication is to be construed as granting any right, by implication or otherwise, for the manufacture, sale, or use of any method, apparatus, or product covered by letters patent. Neither should anything contained in the publication be construed as insuring anyone against liability for infringement of letters patent.

Suggested revisions are invited and should be submitted to the Director of Regulatory Analysis and Scientific Affairs, API, 1220 L Street, NW, Washington, D.C. 20005.

Contents

Figures

Contents

Contents

Simulating the Effect of Aerobic Biodegradation on Soil Vapor Intrusion into Buildings:

Evaluation of Low Strength Sources Associated with Dissolved Gasoline Plumes

Abstract

Aerobic biodegradation can contribute significantly to the attenuation of petroleum hydrocarbon vapors in the unsaturated zone; however, most regulatory guidance for assessing potential human health risks via vapor intrusion to indoor air either neglect biodegradation or only allow for one order of magnitude additional attenuation for aerobically degradable compounds, which may be overly conservative in many cases. This paper describes results from 3-dimensional numerical model simulations of vapor intrusion for petroleum hydrocarbons to assess the influence of aerobic biodegradation on the attenuation factor for a variety of source concentrations and depths for buildings with basements and slab-on-grade construction. Provided that oxygen is present in the vadose zone, aerobic biodegradation of petroleum hydrocarbon vapors in the unsaturated zone will reduce the soil gas concentrations and the potential risks from vapor intrusion to indoor air compared to non-degrading compounds. At lower source concentrations and/or deeper source depths, aerobic biodegradation may result in a reduction in vapor intrusion attenuation factors by many orders of magnitude. The magnitude of the reduction depends on site-specific conditions, which should be considered in the development of a conceptual site model for each site. However, oxygen supply and degradation rates are likely to be sufficient at many sites to mitigate potential risks from vapor intrusion for low vapor concentration sources (less than about 2 mg/L-vapor total hydrocarbons). The simulations conducted in this study provide a framework for understanding the degree to which bio-attenuation will occur under a variety of scenarios and provide insight into site conditions that will result in significant biodegradation. This improved understanding may be used to select site-specific attenuation factors for degradable compounds and develop soil vapor screening levels appropriate for particular combinations of source concentrations, source depth, and building characteristics, which should be defined as part of a site conceptual model.

1. Introduction

Subsurface migration of volatile compounds and vapor intrusion to indoor air is a potential exposure pathway for human occupants of buildings over or near contaminated soils and groundwater. In the past decade, there has been a significant increase in attention to vapor intrusion issues and several new regulatory guidance documents have been developed by State and Federal agencies for assessment and management of vapor intrusion risks. These guidance documents generally provide a framework for screening sites to assess whether vapor intrusion poses no significant risk or may require further evaluation, including assessment, remediation, or exposure controls.

Most regulatory guidance documents use conservative assumptions to account for uncertainties in the screening process. This results in decisions to further evaluate sites more frequently than may actually be necessary. It is expected that screening procedures will become less conservative as we learn more about the processes affecting vapor intrusion. To date, most vapor intrusion screening procedures either assume that biodegradation does not occur, or allow for an arbitrary 10-fold reduction in the predicted indoor air concentration for petroleum hydrocarbons.

Many petroleum hydrocarbons are metabolized by ubiquitous, naturally occurring soil microbes provided that sufficient oxygen is present in the subsurface. Several modeling studies and empirical data reviews have shown that aerobic biodegradation in the unsaturated zone can significantly attenuate vapor intrusion of petroleum hydrocarbons in some settings (i.e. DeVaull, 2007; Abreu and Johnson, 2006, Roggemans, et al. 2001). For example, the Abreu and Johnson (2006) study showed significant reduction in vapor intrusion for deeper and weaker sources and little to no reduction for shallower and stronger sources.

This work builds on the Abreu and Johnson (2006) study by focusing specifically on low-concentration petroleum hydrocarbon vapor sources, as this may be a common case for buildings down-gradient of petroleum source zones and overlying dissolved petroleum hydrocarbon plumes. Simulations were performed using the three-dimensional mathematical model developed by Abreu and Johnson (2006, 2005) for a range of scenarios to develop relationships between the site-specific conditions and the vapor intrusion attenuation factor α, which is defined as the ratio of the indoor air concentration of a chemical divided by its subsurface

vapor source concentration. This mathematical modeling study is intended to provide insight to the significance of bio-attenuation for a wide range of scenarios. It is anticipated that the results may be used to revise regulatory guidance for assessing vapor intrusion to buildings at dissolved petroleum hydrocarbon-impacted sites.

2. Background

Abreu and Johnson (2006) simulated steady-state vapor intrusion scenarios for aerobically biodegradable chemicals using a three-dimensional multi-component transient numerical model. The simulations conducted in their work include a variety of different source concentrations and depths beneath typical residential buildings in simplified geologic settings. These simulations indicate that aerobic degradation rates are likely to be sufficient to degrade hydrocarbons below levels of potential concern to human health via vapor intrusion for sources of sufficient depth beneath the building or where the source concentrations are low (e.g. concentration typical of most dissolved petroleum groundwater plumes).

The development and use of the numerical model is described in detail in Abreu and Johnson (2005, 2006) and Abreu (2005). In brief, the numerical model simultaneously solves transient equations for the soil gas pressure field (from which the advective flow field is computed), transient advective and diffusive transport and reaction of multiple chemicals (including oxygen) in the subsurface, flow and chemical transport through foundation cracks and dilution within the building ventilation. The advective transport is a result of the pressure difference between the building and atmospheric pressures. Although not considered in this study, this code also allows simulations of time-varying atmospheric and indoor pressures. Inputs to the model include geometry descriptors (building footprint, foundation depth, crack locations and widths, source depth, etc.), chemical properties, kinetic parameters, the indoor-outdoor pressure differential, oxygen concentration at ground surface, and the chemical vapor concentration(s) at the vapor source. The model uses a finite-difference numerical method to solve the model partial differential equations and boundary conditions. The numerical accuracy of the code has been demonstrated through the comparison of model predictions with other analytical and numerical model results, and the code has been shown to be capable of fitting field-measured vertical soil gas profiles.

Abreu and Johnson (2006) presented their results as vapor intrusion attenuation factors. Results for vapor source concentration of 2 mg/L showed that vapor attenuation factors for biodegradable compounds could be at least 3 to 18 orders of magnitude less than the no degradation scenarios. This increased attenuation due to biodegradation is significant; however, the magnitude of the effect is sensitive to site-specific conditions. Consequently, a more comprehensive evaluation of the effect of biodegradation on the vapor intrusion pathway is warranted.

3. Approach

The site-specific conditions and the physical settings considered were selected to cover a wide range of potential conditions that might be encountered at hydrocarbon release sites. The conceptual model for the simulations represents typical residential homes with an aerially extensive source directly beneath the building (i.e. lateral separation between the source and the building was not considered). Both basement and slab-on-grade construction scenarios were considered and foundation cracks were assumed to be present around the perimeter of the 10 m $\times$ 10 m structure. Examples of the model domain for each foundation scenario are presented in Figures 1 and 2.

Three key parameters were selected for this evaluation because they are considered to have the most significant influence on bio-attenuation:

- vapor source concentration,
- source depth, and
- biodegradation rates.

A series of model simulations were performed over a range of values for these parameters to generate sufficient information to assess the expected relationship between the attenuation factor and the various site conditions. Homogeneous soil properties and steady-state conditions were simulated in this application of the model.

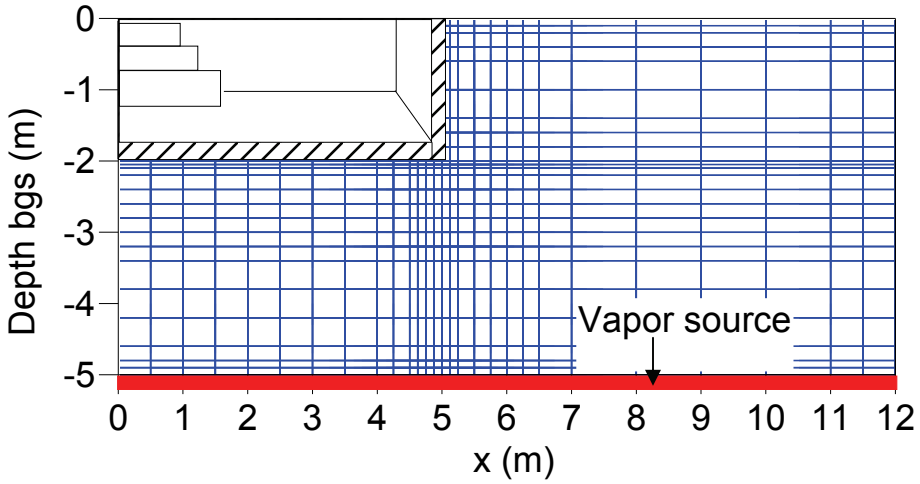

Figure 1—Vertical cross section of sample model domain showing the grid refinement for basement scenario

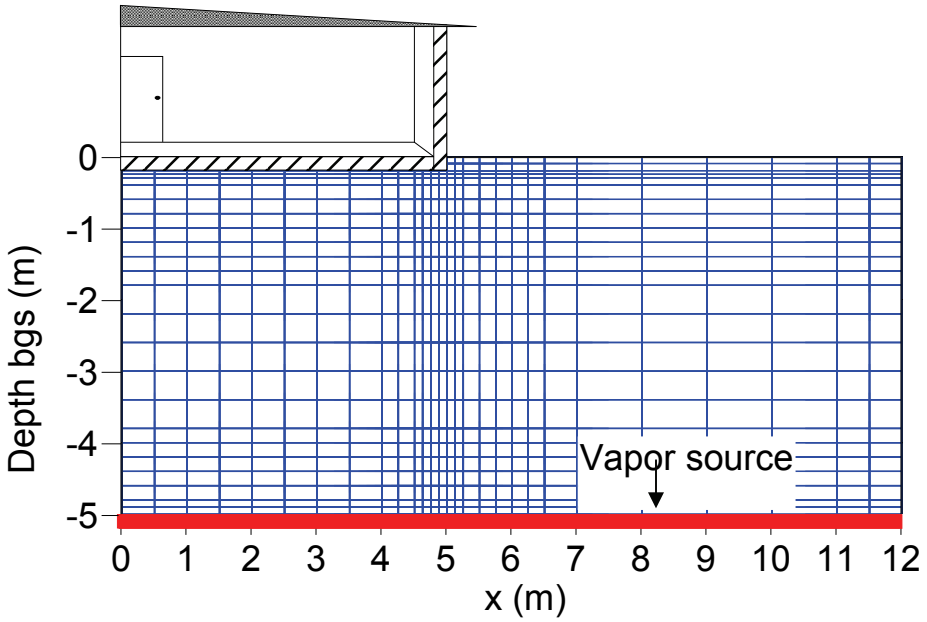

Figure 2—Vertical cross section of sample model domain showing the grid refinement for slab-on-grade scenario

3.1 Conditions Simulated

Unless otherwise specified in the text and figures, the model input parameters common to all simulations are listed in Table 1. These parameter values are the same as those used in Abreu and Johnson (2006) with some exceptions listed below. The sensitivities of the three key parameters were evaluated using values that span typical ranges for each parameter as listed in Table 2.

3.1.1 Vapor Source Concentration

The vapor source concentrations considered in this study ranged from 0.004 to 400 mg/L-vapor. This represents groundwater concentrations ranging from low concentration dissolved phase plumes to concentrations in equilibrium with non-aqueous phase liquid (NAPL) sources. The physical properties for benzene were used in all simulations for single-component source.

Table 1—Model Input Parameters
(unless otherwise noted in the text or figures)

Building/foundation parameters Length: 10 m Width: 10 m Depth in soil: • 2.0 m (basement type) • 0.2 m (slab-on-grade type) Foundation thickness: 0.15 m Enclosed space volume: 244 m^3 Indoor air mixing height: 2.44 m Air exchange rate: 0.5 h^{-1} Crack width: 0.001 m Total crack length: 39 m Crack location: • Perimeter Disturbance pressure: 5 Pa **Soil Properties** Homogeneous sandy soil Soil bulk density: 1660 kg/m^3 Moisture-filled porosity: 0.054 m^3_{water}/m^3_{soil} Total soil porosity: 0.375 m^3_{voids}/m^3_{soil} Soil gas permeability: 10^{-11} m^2 **Soil domain[a] dimensions in (x,y,z) directions** • 12 m × 12 m × (1 to 12 m depths)	**Hydrocarbon vapor source properties** Location: base of vadose zone Source size: entire domain footprint **Hydrocarbon properties** Overall effective diffusion coefficient for transport in the porous media: 5.12E-3 m^2/h Overall effective diffusion coefficient for transport in the crack: 3.17E-2 m^2/h Atmospheric concentration: 0.0 $\mu g/m^3$ **Oxygen properties** Overall effective diffusion coefficient for transport in porous media: 1.16E-2 m^2/h Overall effective diffusion coefficient for transport in the crack: 7.2E-2 m^2/h Ratio of oxygen to hydrocarbon consumed: • 3 kg-oxygen/kg-hydrocarbon Threshold concentration: 1 % vol/vol Atmospheric concentration: 21 % vol/vol **Others** Dynamic viscosity of air: 0.0648 Kg/m/h
[a] The symmetrical scenario domain includes only a quarter of the building footprint (5 m × 5 m footprint area) in the simulation.	

Table 2—Values for Key Parameters Studied

Vapor source concentration (mg/L)	0.004, 0.04, 0.4, 1, 4, 10, 40, 100, 200, 400
Vapor source-foundation separation (m)	1, 2, 3, 4, 5, 7, 10
First-order biodegradation rate constant (1/h)	0 (no biodegradation case), 0.079, 0.79, 2

3.1.2 Depth of Source Below the Building Foundation

The depth of the source below the building foundation ranged from 1 to 10 meters (m). This encompasses a range of shallow source depths that is of interest for most vapor intrusion investigations.

3.1.3 Biodegradation Rates

DeVaull (2007) compiled a total of 84 data sets of reported laboratory and field calculated biodegradation rates for aromatic hydrocarbons measured by multiple investigators. The data included biodegradation rates for individual chemicals: benzene, toluene, ethylbenzene and xylene (BTEX), trimethylbenzene, and naphthalene; as well as rates for mixed BTEX chemicals. The geometric mean of the water-phase first-order biodegradation rates (λ) for the values reported in those studies is 0.79 h^{-1}. The values of λ considered in this work are: 0.079, 0.79 and 2 h^{-1}. These values were selected based on the geometric mean value reported by DeVaull with higher and lower values included to assess the sensitivity of this parameter. The no-biodegradation case ($\lambda = 0$) was also included in this work for comparison purposes.

The oxygen threshold air concentration for biodegradation to occur is a user-defined input to the model. In this study, the oxygen threshold was assumed to be 1 % vol/vol (normalized concentration equal to 0.05). This threshold was chosen based on previous published biodegradation studies. Field data reported in Roggemans, et al. (2001) show decreasing oxygen concentration with depth until reaching a constant value of 2 % vol/vol. Additionally, Bordon and Bedient (1986) report that aerobic biodegradation is observed when the oxygen concentration in groundwater is above 0.1 mg/L-water (vapor equilibrium oxygen concentration of 0.24 % vol/vol). In practice, it is difficult to accurately measure very low oxygen concentrations, and it is

possible that the threshold is below these reported values. If microorganisms can degrade hydrocarbons in the presence of less than 1 % oxygen, then these simulations would underestimate the influence of bio-attenuation.

These simulations also assume that there are no other natural oxygen demands in the vadose zone soils (i.e. oxygen is consumed only by hydrocarbon biodegradation). Therefore, the simulations may overestimate the effect of biodegradation if organic-rich soils are present and their natural demands on oxygen reduce the oxygen concentrations below the levels needed for the biodegradation to occur.

3.2 Multi-Component Mixture Vapor Source

Petroleum hydrocarbon releases are typically mixtures of many aerobically biodegradable compounds, so the migration and bio-attenuation of individual constituents may be affected by the presence of the other compounds in soil vapor. This is expected to be significant due to competition for the oxygen available for biodegradation. Therefore, a set of simulations was also performed using a multi-component vapor source. The composition of a weathered gasoline described by Johnson et al. (1990) was selected for modeling. To facilitate the calculations, the gasoline composition was grouped into seven hydrocarbon constituents/fractions following the approach presented by the Total Petroleum Hydrocarbon Criteria Working Group (TPHCWG, 1997). The source vapor concentration was calculated for two cases: (1) vapor concentrations in equilibrium with a NAPL source and (2) vapor concentrations in equilibrium with a dissolved gasoline plume.

The source vapor composition in equilibrium with a NAPL source scenario was calculated using Raoult's Law. To determine the hydrocarbon composition for the dissolved phase source scenario, a leaching calculation was performed following the approach included in the EPA Soil Screening Guidance (USEPA, 1996). The leaching calculations were based on equilibrium partitioning between sorbed, vapor and aqueous phase. The groundwater source concentration was determined by applying a dilution factor to the calculated leachate concentrations. The vapor source concentrations were calculated from the groundwater concentrations assuming Henry's Law partitioning.

Both types of multiple compounds sources (i.e. NAPL and dissolved plumes) were used in simulations to assess the expected attenuation factors and oxygen consumption (or availability). The compositions of the assumed multi-component sources used in the simulations are presented in Table 3. The biodegradation rates for aromatics and for aliphatics groups of hydrocarbons in the multi-compound mixture were chosen based on the geometric mean values published by DeVaull (2007). For aromatics, a biodegradation rate of 0.79 hr^{-1} was used and for aliphatic compounds, a biodegradation rate of 71 hr^{-1} was used.

Table 3—Multiple Compound Mixture Vapor Source

Weathered Gasoline	Vapor Source Concentration (mg/L)		Henry's Law Constant	First Order Biodegradation Rate	Oxygen Hydrocarbon Ratio
Group/component	Dissolved GW Source	NAPL Source		(1/h)	(g-oxy/g-HC)
Benzene	0.03	0.68	0.228	0.79	3
Toluene	0.40	3.99	0.27	0.79	3
Ethylbenzene	0.11	0.53	0.32	0.79	3
Xylenes	0.61	2.7	0.3	0.79	3
Other Aromatics	1.79	16.4	0.27	0.79	3
Aliphatic C5-C8	32.45	255	86	71	3.5
Aliphatic C9-C12	4.65	5.3	290	71	3.5
SUM	40	285	-	-	-

GW = Groundwater

4. Results and Discussion

The results show the expected effect of biodegradation on the attenuation factor and sub-surface distribution of hydrocarbons and oxygen for a wide variety of scenarios, which should encompass the majority of conditions encountered in vapor intrusion assessments. The results for a source consisting of a single compound are presented first, followed by the results for a multi-component source.

The three-dimensional model output illustrating the hydrocarbon and oxygen soil vapor concentrations distribution is presented as two-dimensional contour plots on vertical cross-sections through the center of the building. In these plots, hydrocarbon concentrations are normalized by the source zone vapor concentration and oxygen concentrations are normalized by atmospheric oxygen concentration (i.e. 21 % vol/vol).

Results and discussion on the predicted soil gas pressure field and the resultant air flow rate into the building predicted for the scenarios studied in this work are presented in Appendix A.

The predicted vapor intrusion attenuation factors for the scenarios studied with a single compound source are presented in Tables 4 and 5 for the basement and slab-on-grade scenarios, respectively. Plots showing the dependence of the attenuation factor on source concentration, source depth, biodegradation rates and building foundation type are presented in Appendices B and C. Details of the effects of these parameters on the bio-attenuation for the vapor intrusion pathway are discussed below.

4.1 Effect of Source Concentration

Soil gas concentration distributions and attenuation factors for hydrocarbon undergoing biodegradation with a first-order biodegradation rate of $\lambda = 0.79\ h^{-1}$ and vapor source concentrations of 0.1, 1 and 10 mg/L are shown in Figure 3 for basement scenarios and in Figure 4 for slab-on-grade scenarios. These source concentrations were selected in order to represent dissolved groundwater plumes at various concentrations below the solubility limit, and multiplied by Henry's Constant to generate a soil gas concentration, assuming equilibrium partitioning between shallow groundwater and deep soil gas. Several concentrations were simulated for a source depth of 5 m bgs. For both the basement and slab-on-grade scenarios, the predicted oxygen concentration beneath the building is sufficient to promote biodegradation and the predicted α-values are about 5.5E-10 and 4.1E-14, respectively. These values are several orders of magnitude lower than the calculated attenuation factors for the no degradation scenarios (α-factor = 1.1E-3 and 6.3E-4 for the basement and slab-on-grade scenarios, respectively). These calculations show 6 to 10 orders of magnitude attenuation attributable to biodegradation, which is much greater than the zero or one order of magnitude assumed currently in regulatory guidance documents.

Figures 3 and 4 show that for vapor source concentrations ranging from 0.1 to 10 mg/L at a depth of 5 m bgs in homogeneous soil, the model predicts oxygen-rich conditions (normalized oxygen concentrations greater than 0.05) beneath the entire building footprint; and biodegradation occurs without oxygen limitations throughout the subsurface. Under such conditions the building presence and foundation type (i.e. basement or slab-on-grade) have very little effect on the hydrocarbon soil gas concentration distribution and near-foundation soil gas samples are reasonably representative of sub-slab concentrations.

When comparing predicted α-values for the different building types in Figures 3 and 4, it should be noted that two factors that affect the transport. First, for a source at the same depth below ground surface (bgs), the source-foundation separation distance is different for these two scenarios. Therefore the hydrocarbon vapor transport distance for the basement scenario is smaller than that for the slab-on-grade scenario. Second, the oxygen transport distance for the basement scenario is larger than that for the slab-on-grade scenario. Due to these factors, the hydrocarbon concentration beneath the foundation for the slab-on-grade scenario is less than that for the basement scenario and consequently the α-values for slab-on-grade scenarios in Figure 4 are about four orders of magnitude smaller than for basement scenarios in Figure 3. However, if the attenuation factors are compared based on the separation distance between the source and the floor of the building (see Tables 2 and 3), they are generally within an order of magnitude, which is relatively small compared to the range of attenuation factors simulated.

Table 4—Attenuation Factor Results for Single Component Source Basement Scenarios

Vapor Source Concentration (mg/L)	Biodegradation Rate (1/h)	Vapor Source Depth Below Foundation (m)						
		1	2	3	4	5	7	10
		Equivalent Vapor Source Depth Below Ground Surface (m)						
		3	4	5	6	7	9	12
400	0	1.3E-03	1.3E-03	1.1E-03	1.0E-03	9.1E-04	7.4E-04	5.7E-04
	0.079	1.2E-03	1.0E-03	8.0E-04	6.2E-04	4.7E-04	2.4E-04	6.4E-05
	0.79	1.2E-03	1.0E-03	7.9E-04	6.2E-04	4.6E-04	2.3E-04	3.3E-05
	2	1.2E-03	1.0E-03	7.9E-04	6.2E-04	4.6E-04	2.3E-04	2.9E-05
200	0	-	-	1.1E-03	1.0E-03	9.1E-04	7.4E-04	5.6E-04
	0.079	-	-	5.2E-04	3.1E-04	1.7E-04	2.8E-05	5.0E-07
	0.79	-	-	5.0E-04	2.7E-04	1.1E-04	1.9E-06	8.6E-12
	2	-	-	5.0E-04	2.7E-04	1.0E-04	4.0E-07	4.4E-15
100	0	1.3E-03	1.3E-03	1.1E-03	1.0E-03	9.0E-04	7.4E-04	5.6E-04
	0.079	8.9E-04	4.6E-04	2.0E-04	6.6E-05	1.5E-05	5.2E-07	6.5E-09
	0.79	8.7E-04	3.6E-04	8.7E-05	5.5E-06	7.8E-08	3.6E-12	2.4E-17
	2	8.7E-04	3.5E-04	6.7E-05	1.5E-06	3.2E-09	1.4E-15	9.5E-23
40	0	1.3E-03	1.3E-03	1.1E-03	1.0E-03	9.0E-04	7.4E-04	5.6E-04
	0.079	5.6E-04	1.6E-04	3.2E-05	4.8E-06	8.3E-07	2.7E-08	1.8E-10
	0.79	3.5E-04	1.1E-05	9.0E-08	2.4E-10	2.7E-12	2.8E-16	3.6E-22
	2	3.1E-04	2.2E-06	2.6E-09	2.5E-13	7.5E-16	2.7E-21	1.5E-29
10	0	1.3E-03	1.3E-03	1.1E-03	1.0E-03	9.0E-04	7.4E-04	5.6E-04
	0.079	4.4E-04	8.0E-05	1.3E-05	2.1E-06	3.4E-07	8.3E-09	3.1E-11
	0.79	1.5E-05	6.8E-08	5.9E-10	2.3E-12	2.3E-14	1.2E-18	2.8E-25
	2	1.8E-06	5.8E-10	7.1E-13	2.1E-16	5.8E-19	8.2E-25	-
4	0	1.3E-03	1.3E-03	1.1E-03	1.0E-03	9.0E-04	7.4E-04	5.6E-04
	0.079	4.4E-04	8.0E-05	1.3E-05	2.1E-06	3.4E-07	8.3E-09	3.1E-11
	0.79	1.5E-05	5.8E-08	5.5E-10	1.5E-12	1.0E-14	5.0E-19	7.7E-26
	2	1.1E-06	2.7E-10	6.1E-13	6.8E-17	1.5E-19	1.2E-25	-
1	0	1.3E-03	1.3E-03	1.1E-03	1.0E-03	9.0E-04	-	-
	0.079	4.4E-04	8.0E-05	1.3E-05	2.1E-06	3.4E-07	-	-
	0.79	1.5E-05	5.8E-08	5.5E-10	1.5E-12	1.0E-14	-	-
	2	1.1E-06	2.7E-10	6.1E-13	6.8E-17	1.5E-19	-	-
0.4	0	1.3E-03	1.3E-03	1.1E-03	1.0E-03	9.0E-04	7.4E-04	5.6E-04
	0.079	4.4E-04	8.0E-05	1.3E-05	2.1E-06	3.4E-07	8.3E-09	3.1E-11
	0.79	1.5E-05	5.8E-08	5.5E-10	1.5E-12	1.0E-14	5.0E-19	7.7E-26
	2	1.1E-06	2.7E-10	6.1E-13	6.8E-17	1.5E-19	1.2E-25	-
0.04	0	1.3E-03	1.3E-03	1.1E-03	1.0E-03	9.0E-04	7.4E-04	-
	0.079	4.4E-04	8.0E-05	1.3E-05	2.1E-06	3.4E-07	8.3E-09	-
	0.79	1.5E-05	5.8E-08	5.5E-10	1.5E-12	1.0E-14	5.0E-19	-
	2	1.1E-06	2.7E-10	6.1E-13	6.8E-17	1.5E-19	1.2E-25	-
0.004	0	1.3E-03	1.3E-03	1.1E-03	1.0E-03	-	-	-
	0.079	4.4E-04	8.0E-05	1.3E-05	2.1E-06	-	-	-
	0.79	1.5E-05	5.8E-08	5.5E-10	1.5E-12	-	-	-
	2	1.1E-06	2.7E-10	6.1E-13	6.8E-17	-	-	-

Table 5—Attenuation Factor Results for Single Component Source Slab-on-Grade Scenarios

Vapor Source Concentration (mg/L)	Biodegradation Rate (1/h)	Vapor Source Depth Below Foundation (m)						
		1	2	3	4	5	7	10
		Equivalent Vapor Source Depth Below Ground Surface (m)						
		1	2	3	4	5	7	10
400	0	1.4E-03	1.1E-03	8.7E-04	7.3E-04	6.3E-04	4.8E-04	3.5E-04
	0.079	1.1E-03	6.3E-04	3.8E-04	2.3E-04	1.3E-04	3.4E-05	2.5E-06
	0.79	1.0E-03	5.2E-04	2.6E-04	1.1E-04	4.0E-05	1.9E-06	1.3E-09
	2	1.0E-03	5.1E-04	2.4E-04	8.9E-05	2.6E-05	3.6E-07	1.2E-11
100	0	1.4E-03	1.1E-03	8.7E-04	7.3E-04	6.3E-04	4.8E-04	3.5E-04
	0.079	8.2E-04	2.5E-04	7.0E-05	1.5E-05	3.2E-06	1.6E-07	2.4E-09
	0.79	4.1E-04	2.4E-05	9.0E-07	1.1E-08	1.5E-10	4.3E-14	6.8E-19
	2	3.1E-04	6.8E-06	6.0E-08	1.2E-10	1.9E-13	1.5E-18	4.5E-25
40	0	1.4E-03	1.1E-03	8.7E-04	7.3E-04	6.3E-04	4.8E-04	3.5E-04
	0.079	7.6E-04	1.4E-04	2.6E-05	4.1E-06	7.6E-07	2.3E-08	1.6E-10
	0.79	1.0E-04	1.1E-06	1.3E-08	3.7E-11	9.5E-13	3.9E-17	1.2E-22
	2	4.0E-05	3.9E-08	1.3E-10	8.9E-15	1.3E-16	4.1E-23	2.1E-30
10	0	1.4E-03	1.1E-03	8.7E-04	7.3E-04	6.3E-04	4.8E-04	3.5E-04
	0.079	7.5E-04	1.4E-04	2.3E-05	3.3E-06	5.5E-07	1.2E-08	4.7E-11
	0.79	6.2E-05	3.7E-07	3.0E-09	2.8E-12	4.9E-14	5.2E-19	2.8E-25
	2	8.4E-06	5.5E-09	8.9E-12	1.1E-16	1.1E-18	3.3E-26	-
4	0	1.4E-03	1.1E-03	8.7E-04	7.3E-04	6.3E-04	4.8E-04	3.5E-04
	0.079	7.5E-04	1.4E-04	2.3E-05	3.3E-06	5.5E-07	1.2E-08	4.7E-11
	0.79	6.2E-05	3.7E-07	3.0E-09	2.8E-12	4.1E-14	3.4E-19	1.1E-25
	2	8.4E-06	5.5E-09	8.6E-12	8.1E-17	5.9E-19	1.3E-26	-
1	0	1.4E-03	1.1E-03	8.7E-04	7.3E-04	6.3E-04	4.8E-04	-
	0.079	7.5E-04	1.4E-04	2.3E-05	3.3E-06	5.5E-07	1.2E-08	-
	0.79	6.2E-05	3.7E-07	3.0E-09	2.8E-12	4.1E-14	3.4E-19	-
	2	8.4E-06	5.5E-09	8.6E-12	8.1E-17	5.9E-19	1.2E-26	-
0.4	0	1.4E-03	1.1E-03	8.7E-04	7.3E-04	6.3E-04	4.8E-04	3.5E-04
	0.079	7.5E-04	1.4E-04	2.3E-05	3.3E-06	5.5E-07	1.2E-08	4.7E-11
	0.79	6.2E-05	3.7E-07	3.0E-09	2.8E-12	4.1E-14	3.4E-19	1.0E-25
	2	8.3E-06	5.5E-09	8.6E-12	8.1E-17	6.0E-19	1.2E-26	-
0.04	0	1.4E-03	1.1E-03	8.7E-04	7.3E-04	6.3E-04	4.8E-04	-
	0.079	7.5E-04	1.4E-04	2.3E-05	3.3E-06	5.5E-07	1.2E-08	-
	0.79	6.2E-05	3.7E-07	3.0E-09	2.8E-12	4.1E-14	3.5E-19	-
	2	8.4E-06	5.5E-09	8.6E-12	8.1E-17	5.9E-19	1.2E-26	-
0.004	0	1.4E-03	1.1E-03	8.7E-04	7.3E-04	-	-	-
	0.079	7.5E-04	1.4E-04	2.3E-05	3.3E-06	-	-	-
	0.79	6.2E-05	3.7E-07	3.0E-09	2.8E-12	-	-	-
	2	8.4E-06	5.5E-09	8.6E-12	8.1E-17	-	-	-

For the three scenarios presented in Figures 3 and 4, the attenuation factor is insensitive to source concentration over the range presented. This is a result of oxygen rich conditions throughout the subsurface. However, for scenarios with higher oxygen utilization (e.g. higher hydrocarbon source concentration), the attenuation factor will be dependent on the source concentration. This demonstrates the importance of understanding the oxygen distribution as part of a site assessment for vapor intrusion at petroleum hydrocarbon release sites. The simulations here assume steady-state soil gas flow into the building, and this is a simplification of real-world conditions. If a building has pressure that fluctuates between being higher and lower than the soil gas pressure, then the flux of oxygen to the region beneath the building will increase to some degree, and the oxygen deficient zone may not develop to the same extent. Potential differences in conditions beneath and beside a building should be considered when selecting locations and depths for sample collection.

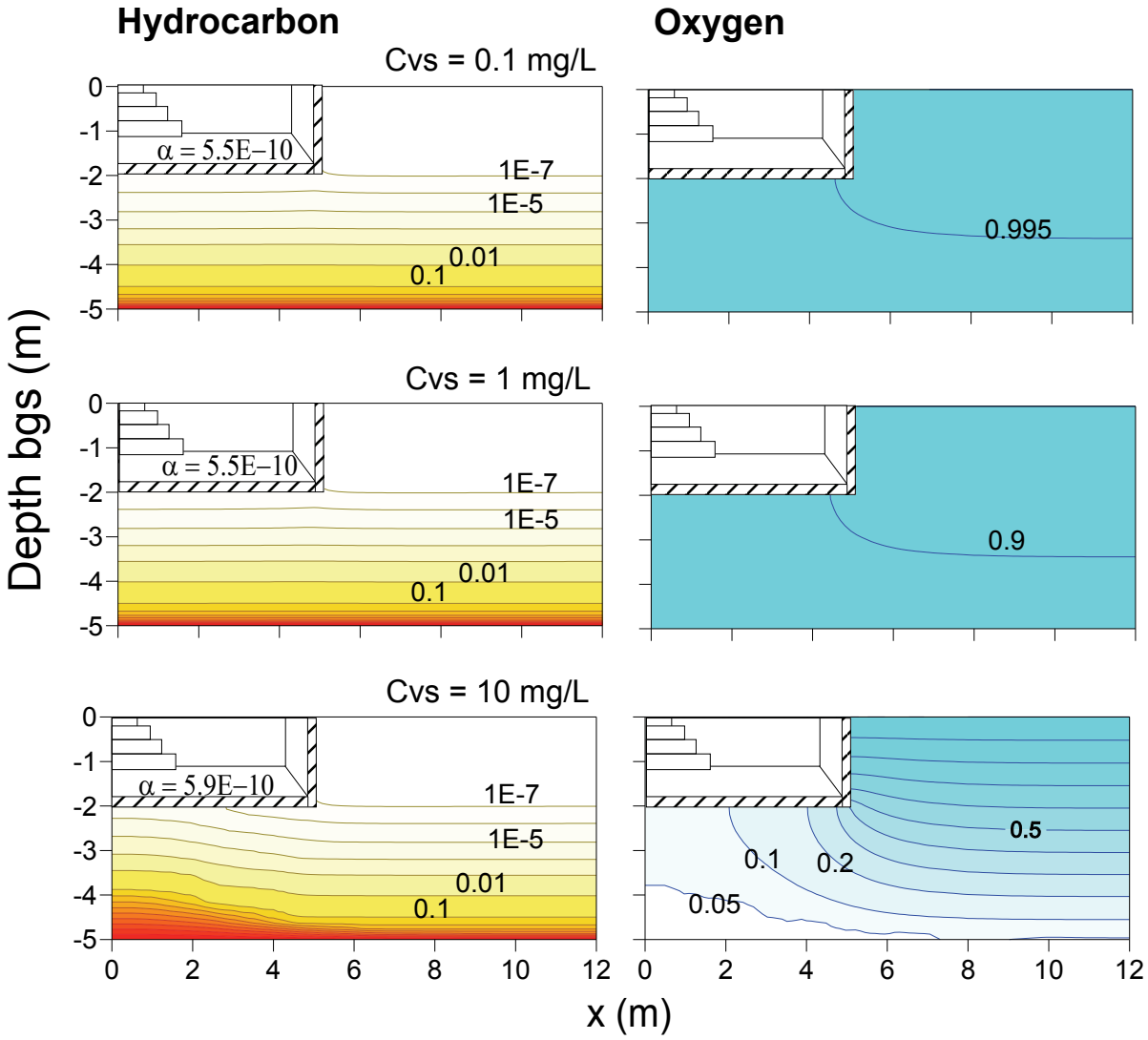

Figure 3—Effect of low vapor source concentration (Cvs) on soil gas concentration distribution and vapor intrusion attenuation factors (α) for basement foundation scenarios and hydrocarbon biodegradation rate $\lambda = 0.79\ h^{-1}$. Hydrocarbon and oxygen concentrations are normalized by source and atmospheric concentrations, respectively.

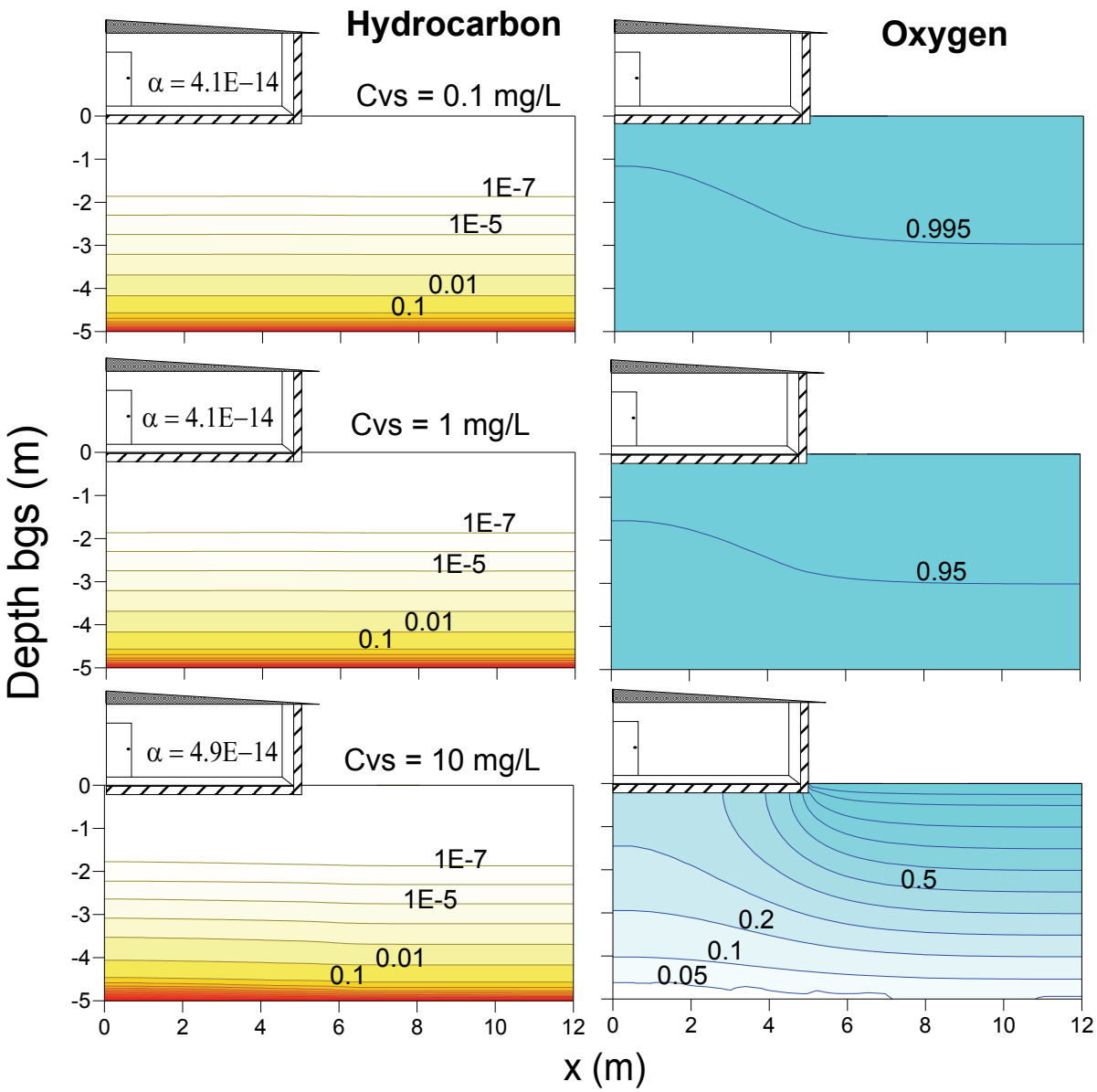

Figure 4—Effect of low vapor source concentration (Cvs) on soil gas concentration distribution and vapor intrusion attenuation factors (α) for slab-on-grade foundation scenarios and hydrocarbon biodegradation rate λ = 0.79 h^{-1}. Hydrocarbon and oxygen concentrations are normalized by source and atmospheric concentrations, respectively.

Vapor intrusion attenuation factors (α) are presented in Figures 5 and 6 for a broader set of source concentrations and first-order biodegradation rates than those shown on Figures 3 and 4. In Figure 5, α is presented as function of source concentration and first-order degradation rates of 0.079, 0.79 and 2 h^{-1} for a basement scenario with source depth of 5 m bgs. Figure 6 presents comparable plots for a slab-on-grade scenario. For reference, each plot shows the predicted curve for the no-biodegradation case. Figures 5 and 6 are similar to ones presented by Abreu and Johnson (2006) and show a family of curves with similar shapes and trends of increasing α-values with increasing vapor source concentration and decreasing biodegradation rates. For very high vapor source concentrations, the α-values approach the no-biodegradation case due to oxygen depletion beneath the foundation. For low vapor source concentration ranges (less than approximately 10 mg/L), α-values are relatively unaffected by changes in hydrocarbon vapor source concentration due to oxygen rich conditions throughout the subsurface (see Figures 3 and 4) and the first-order biodegradation kinetic model.

Figures 5 and 6 and the plots of α-values vs source concentration presented in Appendix B and C for basement and slab-on-grade scenarios, indicate that for low vapor source concentrations (less than approximately 10 mg/L),α-values are not sensitive to the vapor source concentration. Note that these results are for foundation-crack located along the slab perimeter. Previous work (Abreu, 2005) has shown that α-values may be dependent on crack locations for scenarios with homogeneous sandy soil and shallow sources. Implications of crack location and how it affects the general conclusions regarding the dependence of attenuation factors on source concentrations are discussed further in 5.2.

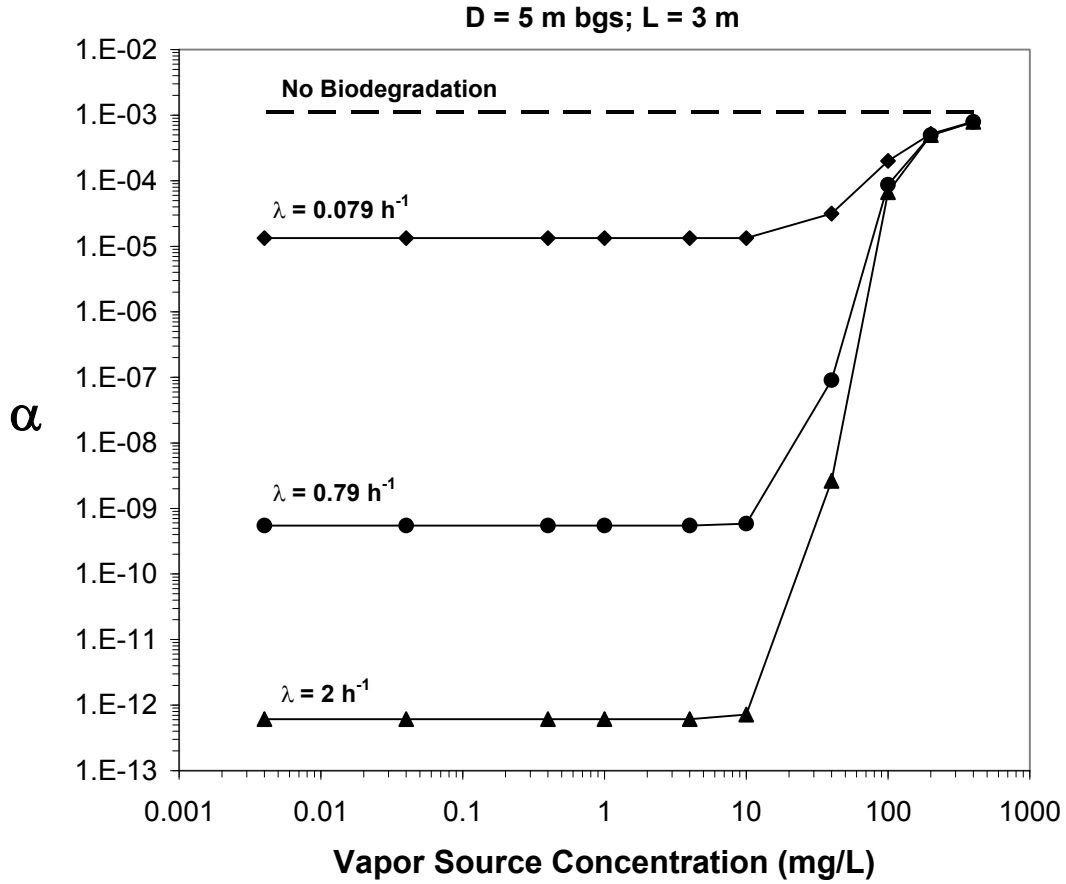

Figure 5—Influence of soil vapor source concentration and first-order biodegradation rates (λ) on vapor intrusion attenuation factors (α) for basement scenarios, homogeneous sand soil and source depth (D) of 5 m bgs (source-foundation separation L = 3 m).

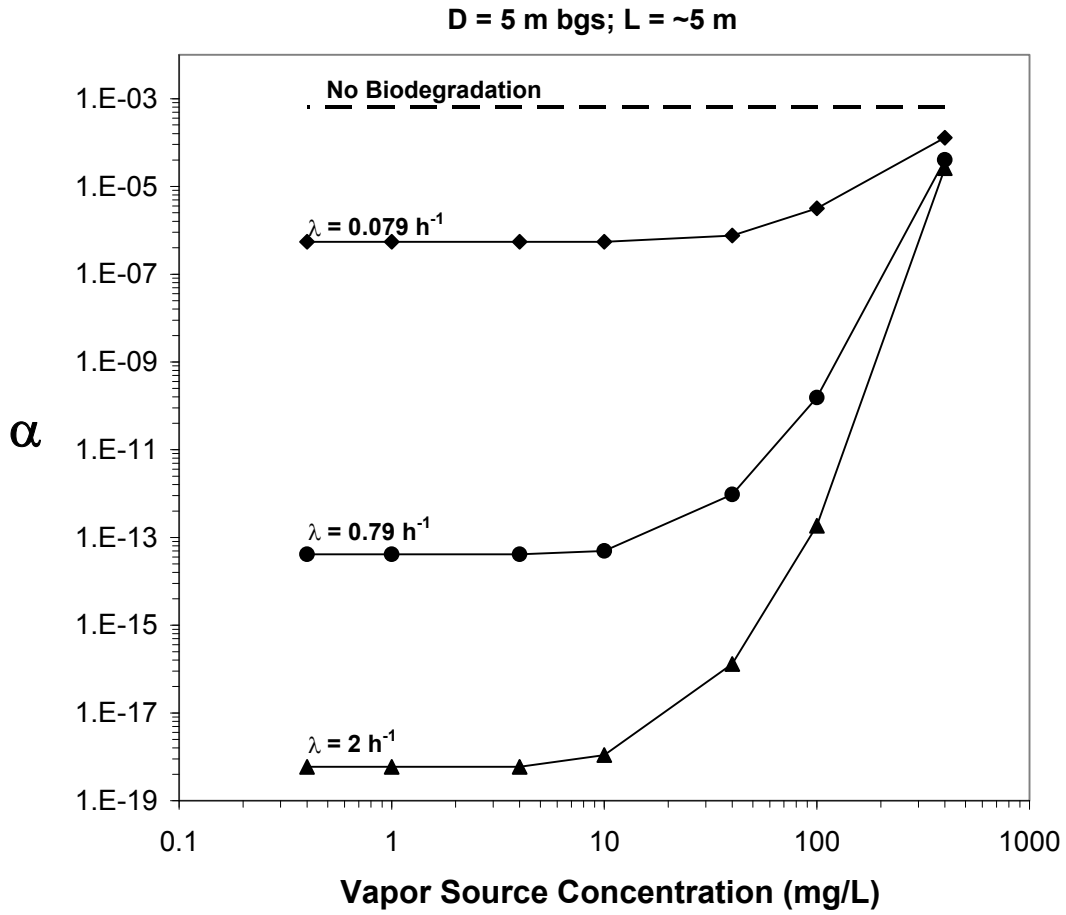

Figure 6—Influence of soil vapor source concentration and first-order biodegradation rates (λ) on vapor intrusion attenuation factors (α) for slab-on-grade scenarios, homogeneous sand soil and source depth (D) of 5 m bgs (source-foundation separation L = ~5 m).

4.2 Effect of First-Order Biodegradation Rate

The effect of first-order biodegradation rates on soil gas concentration profiles for the low source concentration range is illustrated in Figures 7 and 8 for basement and slab-on-grade scenarios, respectively. For these simulations, a vapor source concentration of 4 mg/L located at 4 m bgs was assumed. The hydrocarbon soil gas concentration profiles in Figures 7 and 8 show about 5 orders-of-magnitude reduction in hydrocarbon vapor concentration at about 2 m bgs as λ increases from 0.079 to 2 h^{-1}. Additionally, for the source concentration and depth simulated, the oxygen concentration profiles beneath the slab show increasing oxygen utilization as λ increases. This illustrates the sensitivity of the degradation rate for the vapor intrusion pathway. The α-values decrease about 5 orders-of-magnitude for the basement scenario and about 10 orders-of-magnitude for the slab-on-grade scenario as λ increases from 0.079 to 2 h^{-1}.

4.3 Effect of Source Depth

The effect of source depth on the soil gas concentration distribution for a vapor source concentration of 1 mg/L and a first-order biodegradation rate of 0.79 h^{-1} is illustrated in Figures 9 and 10. Figure 9 shows the results for basement scenarios with sources at 3, 5 and 7 m bgs (corresponding to source-foundation separation of 1, 3 and 5 m). Figure 10 shows the results for slab-on-grade scenarios with sources at 1, 3, 5 and 7 m bgs (corresponding to source-foundation separation of ~1, 3, 5 and 7 m). These simulations indicate multiple orders of magnitude decrease in α-values with an increase in source depth of approximately 2 meters. For these scenarios, oxygen rich conditions (oxygen concentrations > 1 % vol/vol) are present throughout the subsurface, even for very shallow source depths.

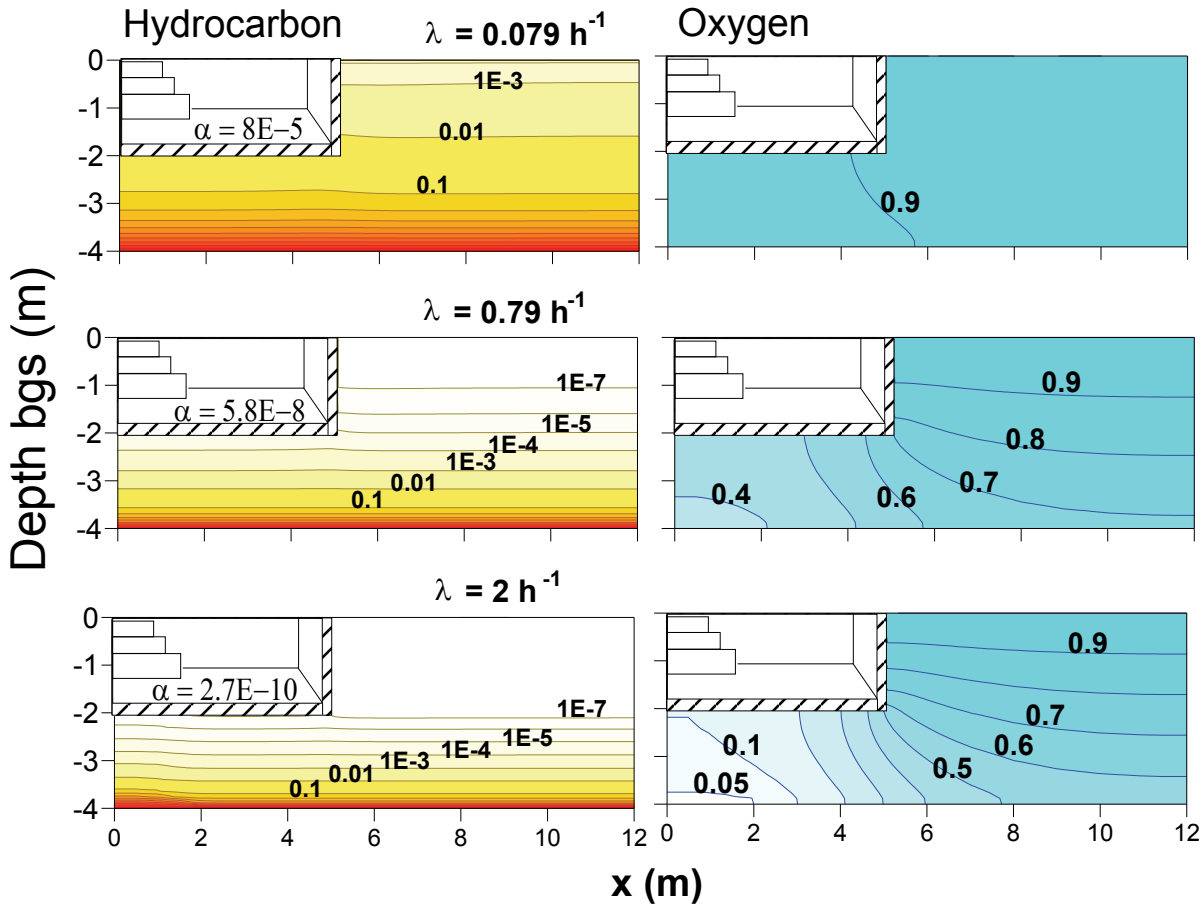

Figure 7—Effect of biodegradation rate (λ on soil gas concentration distribution and vapor intrusion attenuation factors (α) for low vapor source concentration (4 mg/L) located at 4 m bgs (2 m below a basement foundation). Hydrocarbon and oxygen concentrations are normalized by source and atmospheric concentrations, respectively.

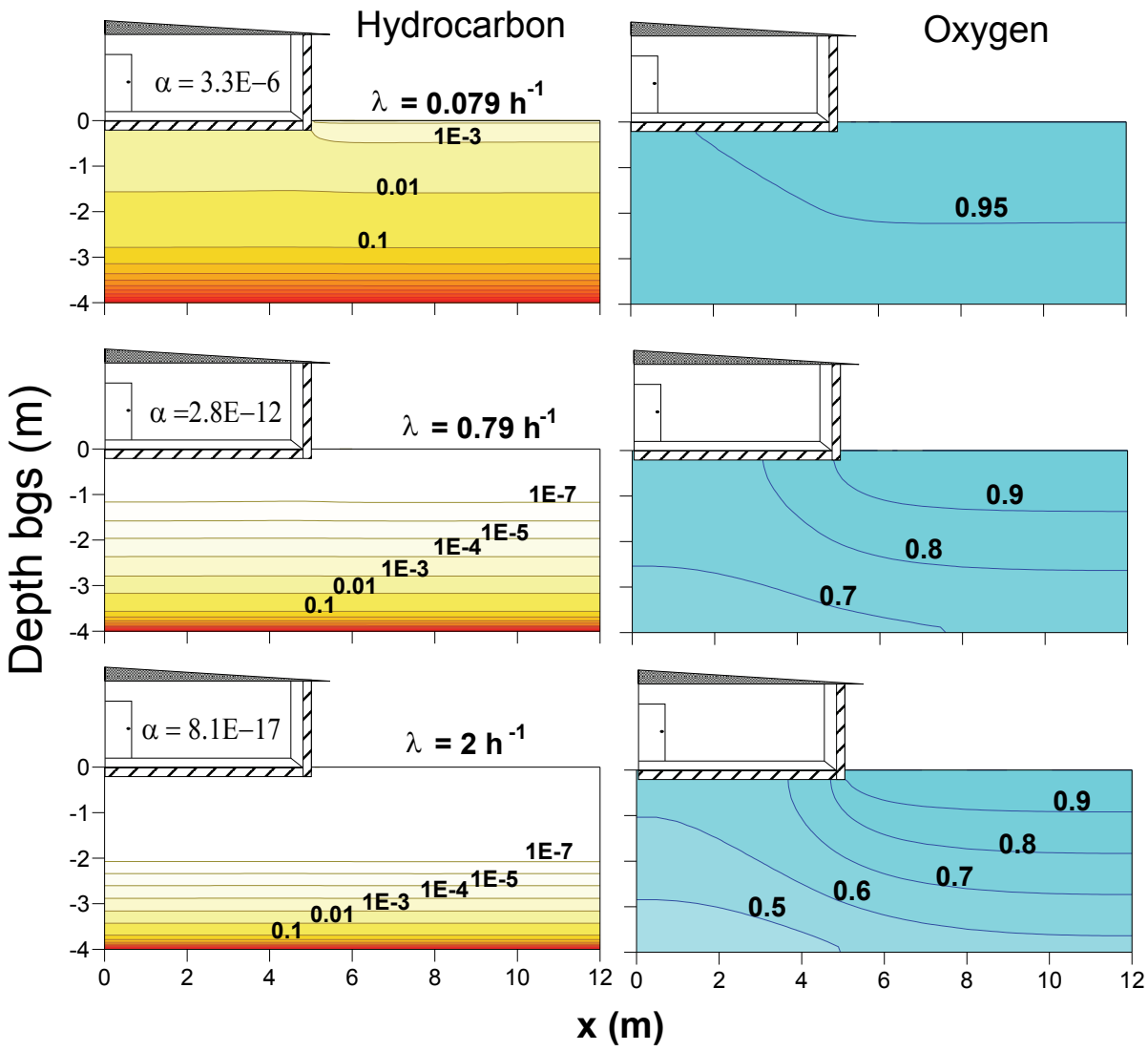

Figure 8—Effect of biodegradation rate (λ on soil gas concentration distribution and vapor intrusion attenuation factors (α) for low vapor source concentration (4 mg/L) located at 4 m bgs (~4 m below the slab-on-grade foundation). Hydrocarbon and oxygen concentrations are normalized by source and atmospheric concentrations, respectively.

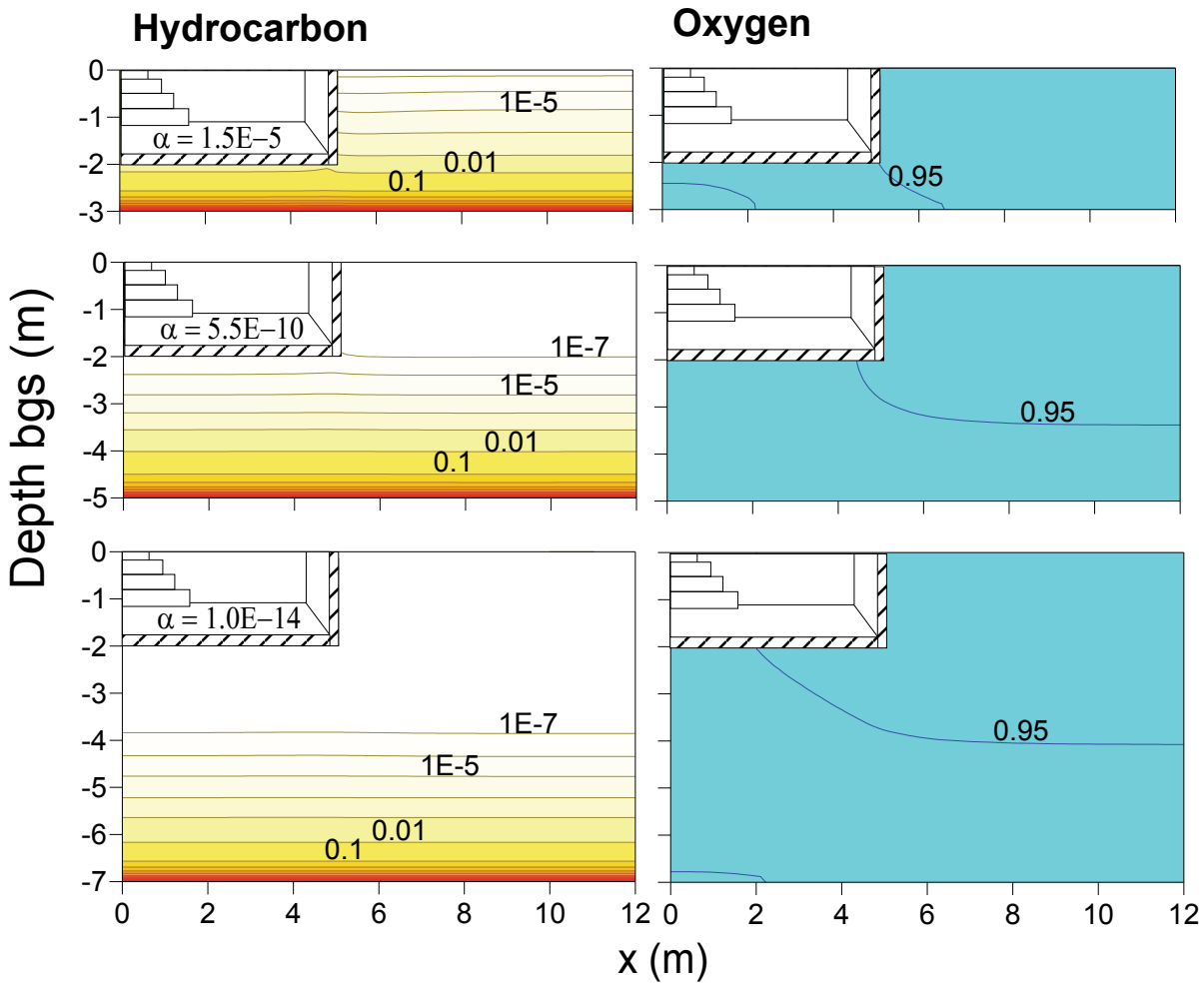

Figure 9—Effect of source depth on the soil gas concentration distribution and vapor intrusion attenuation factors (α) for basement scenarios with a low vapor source concentration of 1 mg/L and biodegradation rate λ = 0.79 h^{-1}. Hydrocarbon and oxygen concentrations are normalized by source and atmospheric concentrations, respectively.

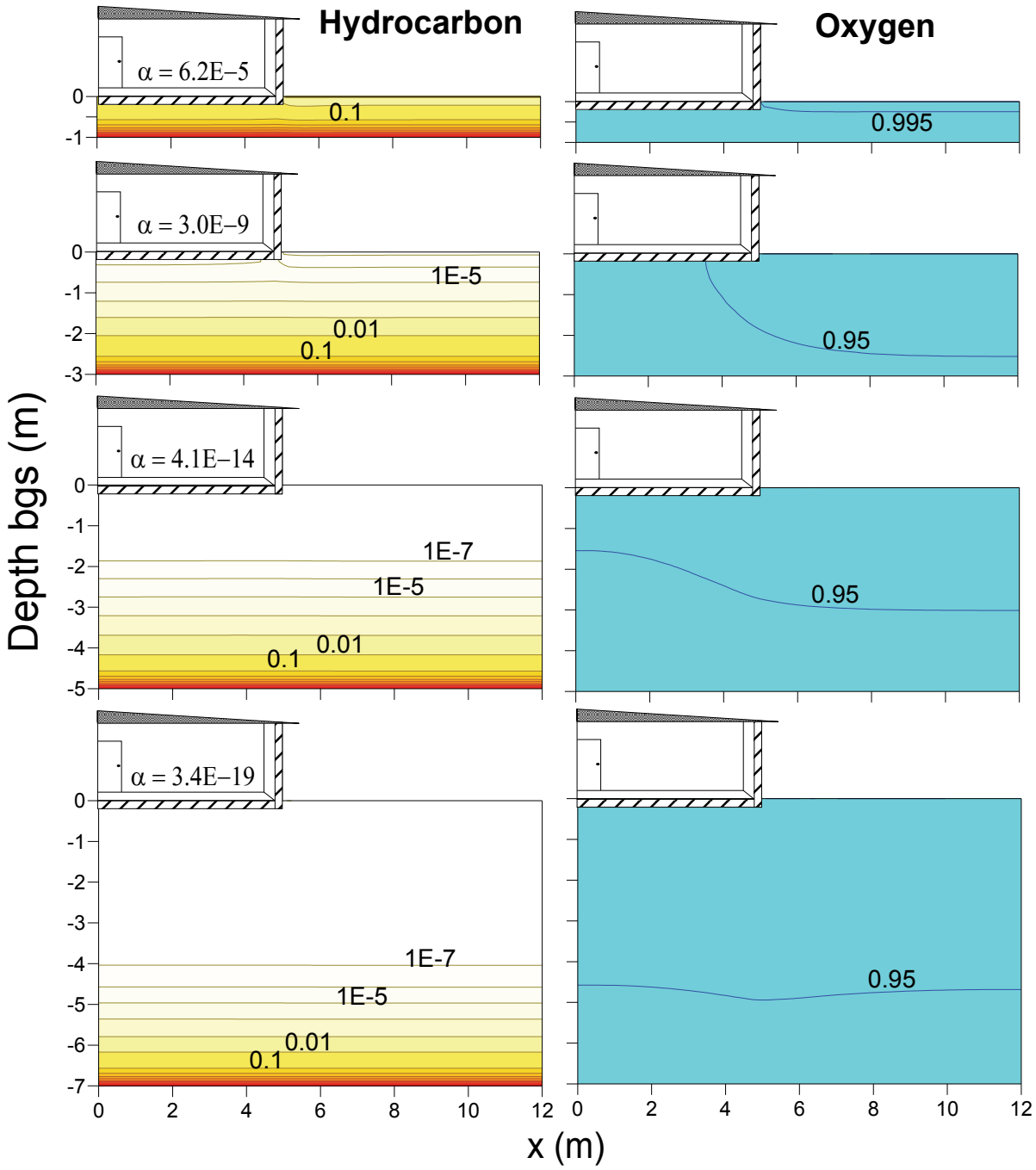

Figure 10—Effect of source depth on the soil gas concentration distribution and vapor intrusion attenuation factors (α) for slab-on-grade scenarios with a low vapor source concentration of 1 mg/L and biodegradation rate $\lambda = 0.79\ h^{-1}$. Hydrocarbon and oxygen concentrations are normalized by source and atmospheric concentrations, respectively.

Note that the effect of source depth on soil gas concentration distribution is expected to be different for high vapor source concentrations. Abreu and Johnson (2006) have shown that for a high vapor source, oxygen penetration beneath the building may be limited for small source-foundation separation. In these cases, the effect of biodegradation on the vapor intrusion pathway may be less significant. Figure 11 presents the normalized soil gas concentration profile for a 100 mg/L vapor source at depths of 3, 7 and 9 m bgs and a basement scenario. Figure 11 indicates oxygen depletion beneath the building as the source-foundation separation becomes smaller. The attenuation factor increases by several orders of magnitude as the amount of biodegradation diminishes. Note that these results are for a homogeneous subsurface and heterogeneities may result in different oxygen and hydrocarbon concentration distribution.

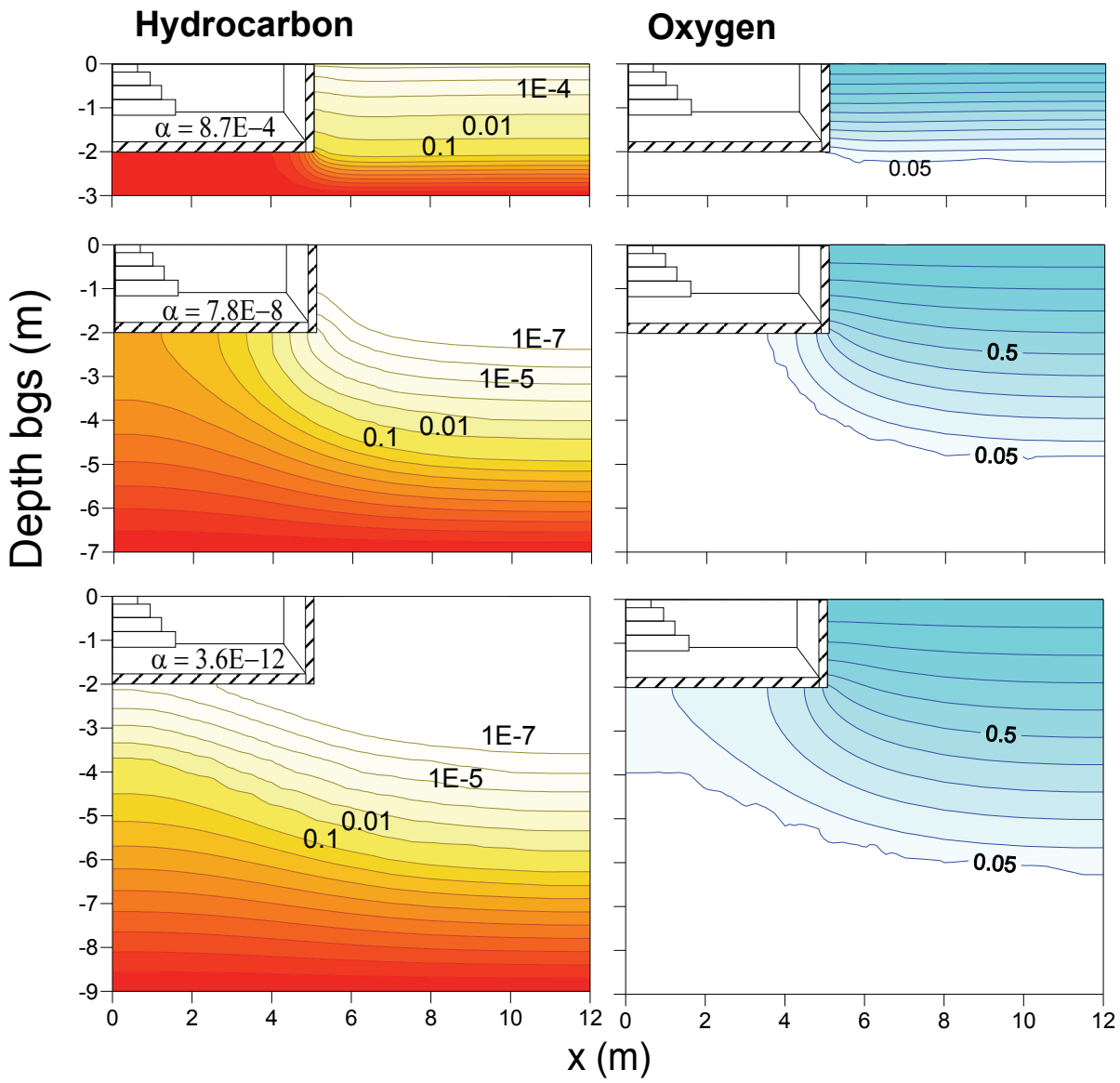

Figure 11—Effect of source depth on the soil gas concentration distribution and vapor intrusion attenuation factors (α) for basement scenarios with a high vapor source concentration of 100 mg/L and biodegradation rate λ = 0.79 h^{-1}. Hydrocarbon and oxygen concentrations are normalized by source and atmospheric concentrations, respectively.

Figures 12 and 13 show the dependence of the vapor intrusion attenuation factor as a function of source depth for the range of biodegradation rates considered in this study. These figures plot the α-values for vapor source concentration of 10 mg/L. Note that these figures show the α-values as a function of depth below the foundation, not depth below ground surface. The no-degradation case is also plotted to show the relative amount of attenuation from biological degradation compared to the no-biodegradation case. For conditions specified in Table 1, the attenuation factors are insensitive to vapor source concentrations below 10 mg/L (as shown on Figures 5 and 6). Therefore, the results presented in Figures 12 and 13 are applicable to scenarios with vapor source concentrations ≤ 10 mg/L.

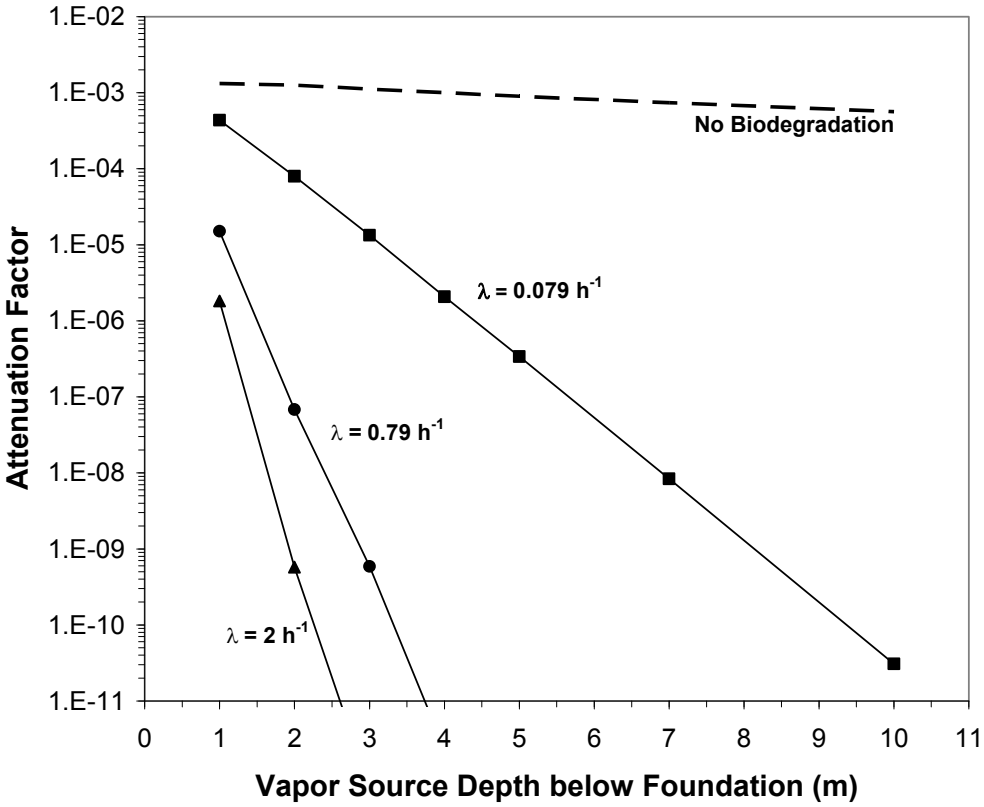

Figure 12—Attenuation factors as a function of source depth below foundation and first-order biodegradation rate for basement scenarios with perimeter cracks and 10 mg/L vapor source concentration. This graph is applicable to all sources with vapor concentration ≤ 10 mg/L.

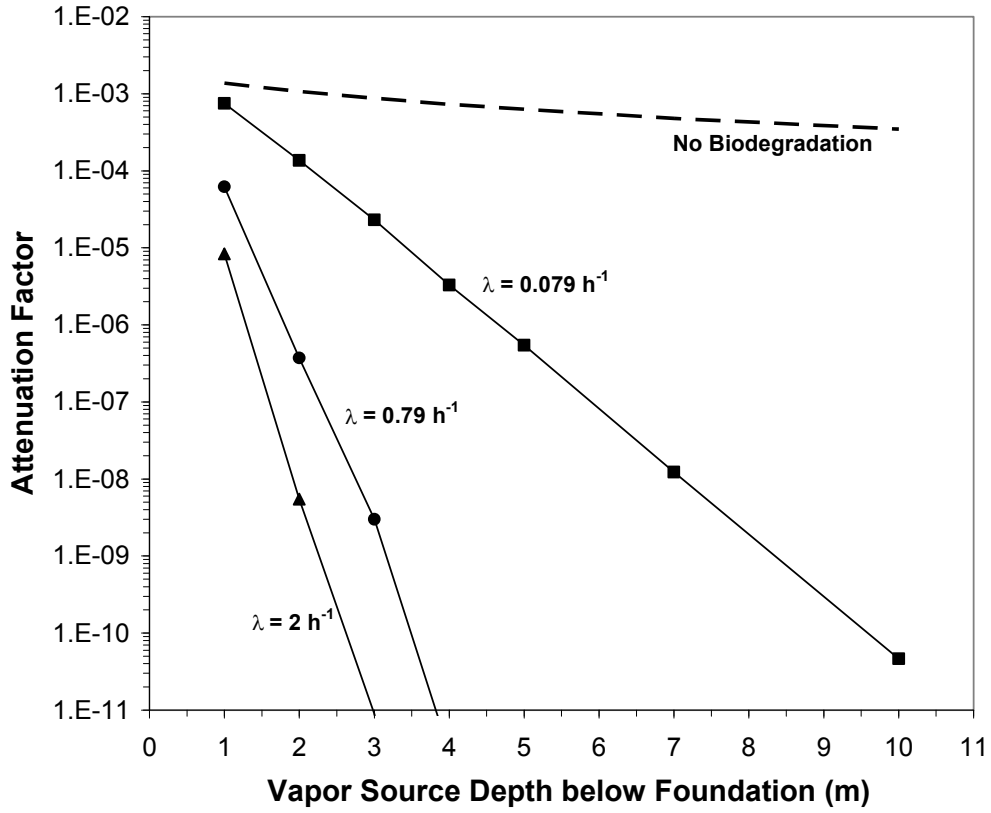

Figure 13—Attenuation factors as a function of source depth below foundation and first-order biodegradation rate for slab-on-grade scenarios with perimeter cracks and 10 mg/L vapor source concentration. This graph is applicable to all sources with vapor concentration ≤ 10 mg/L.

4.4 Effect of Building Type

Figure 14 shows the normalized soil gas concentration profile for a low vapor source concentration of 4 mg/L located 4 m bgs for a basement and a slab-on-grade scenario. The soil gas concentration profiles presented in Figure 14 and in figures above show that for low-concentration vapor sources, oxygen rich conditions allowing for biodegradation are predicted throughout the subsurface. Under these conditions, the building foundation type does not affect the soil gas concentration distribution. These figures also illustrate that for the same source depth below ground surface, slab-on-grade foundation scenarios are expected to have attenuation factors several orders of magnitude smaller than those for basement scenarios. This is primarily a result of the larger source-foundation separation for the slab-on-grade scenarios.

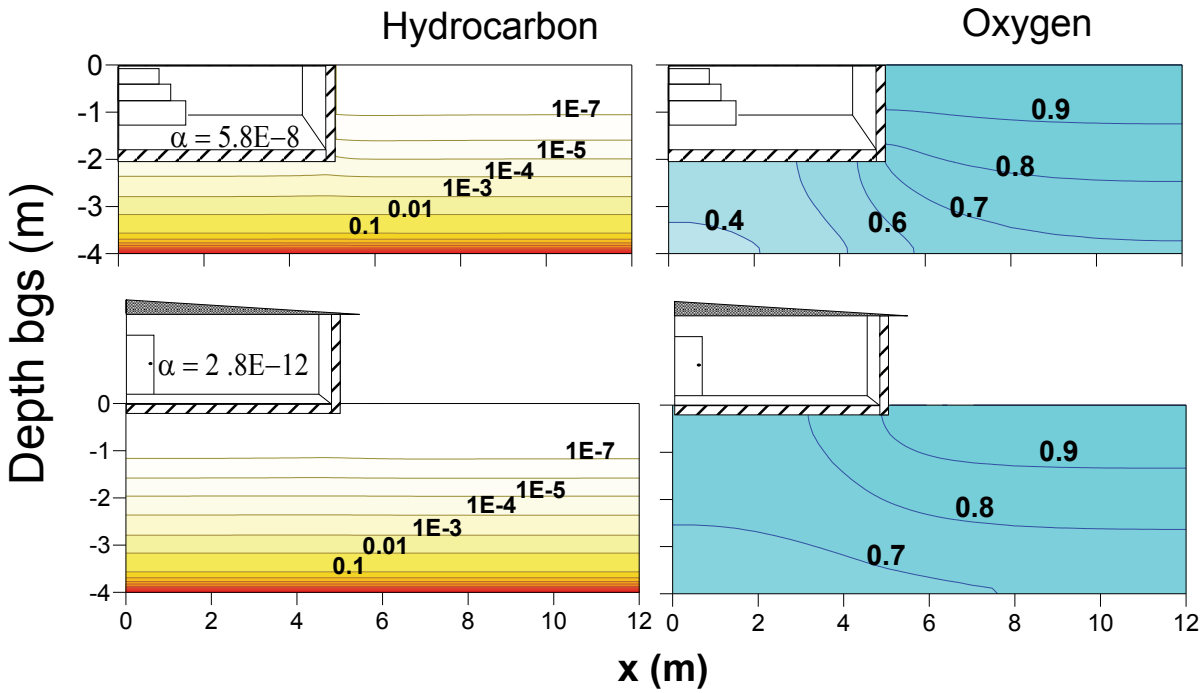

Figure 14—Effect of building type on soil gas concentration distribution for low vapor source concentration (4 mg/L) and biodegradation rate λ = 0.79 h^{-1}. Hydrocarbon and oxygen concentrations are normalized by source and atmospheric concentrations, respectively.

Note that for high concentration sources, greater oxygen consumption occurs and the building structure may affect the oxygen and hydrocarbon distributions in the subsurface (Abreu and Johnson, 2006). Figure 15 presents the normalized soil gas concentration profile for a high concentration vapor source of 100 mg/L located 7 m bgs for basement and slab-on-grade scenario. In Figure 15, it is evident that the effect of the building on the concentration profile is more pronounced for basement foundation scenario. The calculated α-values for the basement and slab-on-grade scenarios are different by more than 6 orders of magnitude.

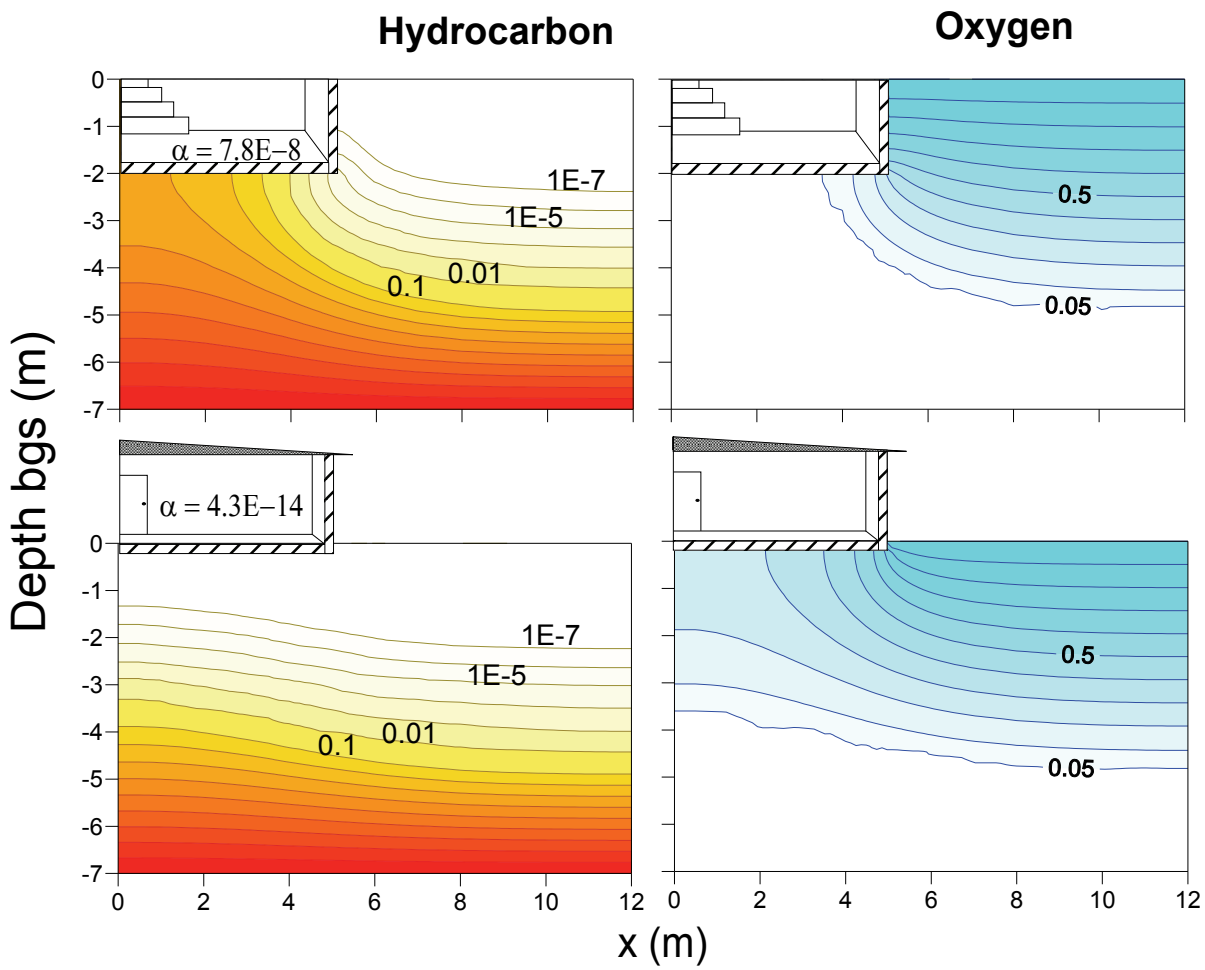

Figure 15—Effect of building type on soil gas concentration distribution for high vapor source concentration (100 mg/L) and biodegradation rate λ = 0.79 h^{-1}. Hydrocarbon and oxygen concentrations are normalized by source and atmospheric concentrations, respectively.

4.5 Results and Discussion for Multi-Component Gasoline Sources

Simulations performed with multi-component sources were conducted using the same model input parameters for the soil and building considered in the single-component source scenarios (i.e. only chemical-specific parameters were varied). As described above, the multi-component source was characterized by assigning concentrations for seven constituent/ fractions to represent a weathered gasoline mixture. The compositions for dissolved phase and NAPL vapor sources are shown in Table 3. Chemical, physical, and biodegradation properties were assigned for each constituent/fraction. This approach permits evaluation of the oxygen consumption resulting from the aerobic biodegradation for each constituent of the multi-component source. The normalized soil gas concentration distributions for a single-component and multi-component sources are compared in Figures 16 and 17 for the dissolved phase and NAPL source scenarios.

Figure 16 shows the soil gas concentration distributions for a vapor source concentration of 40 mg/L-vapor. This concentration represents the total petroleum hydrocarbon (TPH) vapor source resulting from a high concentration weathered gasoline dissolved phase plume (groundwater concentration approximately equal to 11 mg/L-water). The single compound vapor source results presented in this figure are based on a neat benzene source of 40 mg/L-vapor (i.e. not the benzene fraction from the weathered gasoline source). These calculations consider a slab-on-grade foundation with a source depth of 4 m bgs.

Figure 17, shows the soil gas concentration distributions for a vapor source concentration of 285 mg/L-vapor. This concentration represents the TPH vapor source resulting from a weathered gasoline NAPL source. The

single-component vapor source results presented in this figure are based on a neat benzene source of 285 mg/L-vapor. These calculations consider a slab-on-grade foundation with a source depth of 10 m bgs.

The oxygen concentration distribution plots in Figures 16 and 17 show that the total oxygen consumption is similar for the single and multi-component sources. The contour plots also show similar profiles for benzene from a single component source and BTEX and other aromatics for the multi-component source scenarios. This similarity in the aromatic hydrocarbon distribution is a result of similar chemical properties and biodegradation rates for these constituents. The concentration profiles indicate less biodegradation for aliphatic hydrocarbons than for the aromatic hydrocarbons even though the biodegradation rate constants for the aliphatics are higher than those for the aromatic compounds. This is a result of the different gas-water partitioning for these classes of compounds and the initial assumption that biodegradation is occurring only in the dissolved phase. Because the Henry's law coefficient for aliphatics are much higher than those for the aromatics (see Table 3), only a relatively small portion of the total mass of aliphatic hydrocarbons is present in the aqueous phase assumed to be available for biodegradation. Under these assumed conditions the overall consumption of oxygen by the multi-component source is similar to the single compound source for the biodegradation rates used in this study.

Aliphatic hydrocarbons generally degrade faster aerobically than aromatic hydrocarbons, based on available data reviewed to date. DeVaull (2007) reported average degradation rates for aliphatics ranging from 4 to 1,100 hr^{-1}, with a geometric mean of 71 hr^{-1}. For aromatics, reported average degradation rates ranged from 0.4 to 2 hr^{-1}, with a geometric mean of 0.79 hr^{-1}. The vapor concentration profiles simulated in this work have not yet been compared to field measurements for all scenarios, so they may differ from site-specific conditions. Many of the simulated hydrocarbon concentrations are lower than typical laboratory reporting limits, so a direct comparison between the model and field data may not be possible at many sites. For low concentration hydrocarbon sources, the oxygen concentration profiles are not expected to change significantly from those presented in this report with changes in the aliphatic degradation rate constants because oxygen concentrations are typically much higher than the hydrocarbon concentrations, and are therefore less sensitive to changes.

Tables 6 and 7 present the attenuation factors predicted for the scenarios shown in Figures 16 and 17, respectively. The attenuation factors calculated for the aromatic hydrocarbons in the multi-component scenarios are very similar to the attenuation factor for benzene in the single component case. These results indicate that the calculated attenuation factors for the single component simulations may be applicable to the vapor intrusion evaluation for aromatic compounds in multi-component petroleum hydrocarbon sources. Note that the total concentration of all biodegradable species in the multi-component vapor source must be used to select an applicable attenuation factor and not just the concentration of the compound of interest.

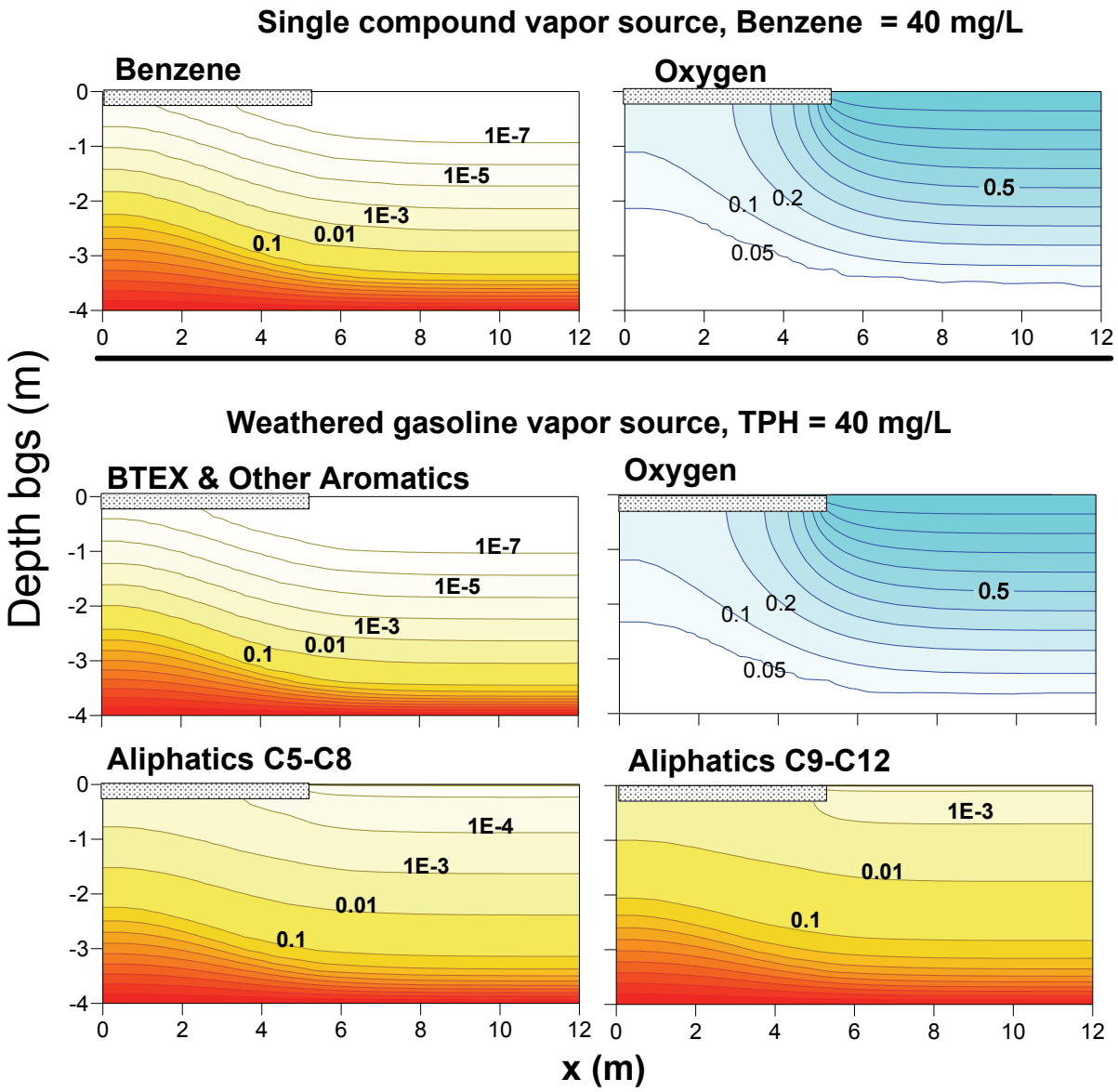

Figure 16—Effect of multi-component source on soil gas distribution and oxygen consumption in the subsurface for dissolved groundwater source scenario. For comparison purposes two source types are illustrated: Single and multi-component sources. Each is located underneath a slab-on-grade scenario at 4 m bgs; and each source has 40 mg/L total vapor concentration.

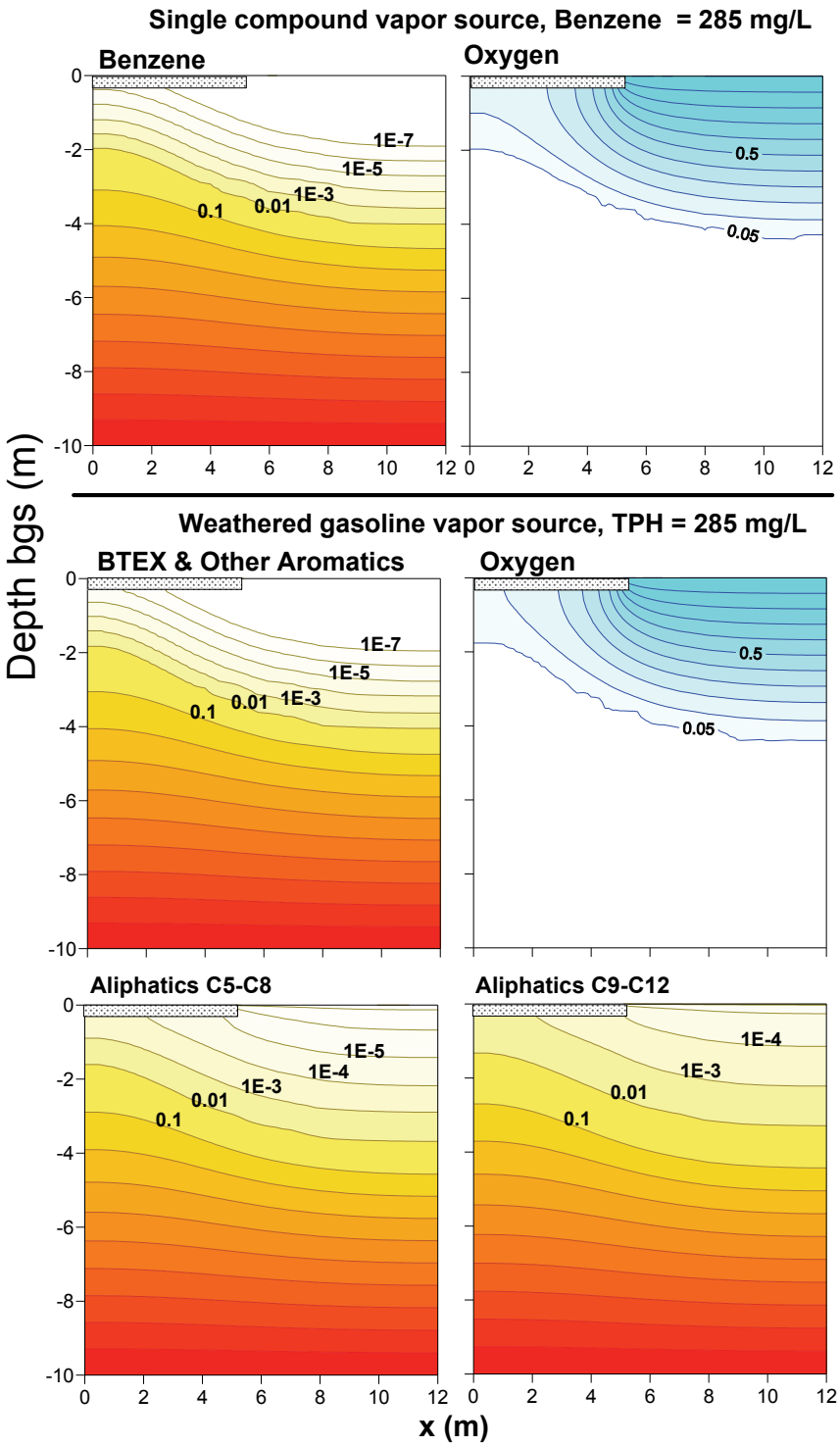

Figure 17—Effect of multi-component source on soil gas distribution and oxygen consumption in the subsurface for NAPL source scenario. For comparison purposes two source types are illustrated: Single and multi-component sources. Each is located underneath a slab-on-grade scenario at 10 m bgs; and each source has 285 mg/L total vapor concentration.

Table 6—Predicted Attenuation Factors for Dissolved Groundwater Multiple-Component Source and Equivalent Single Component Source for Slab-on-Grade Scenario and Source Depth of 4 m bgs

Dissolved Groundwater Multiple-Component Source			
Weathered Gasoline Group/Component	Vapor Source Concentration (mg/L-vapor)	Attenuation Factors	
		No Biodegradation	With Biodegradation
Benzene	0.035	7.3E-04	1.7E-11
Toluene	0.40	7.3E-04	6.1E-11
Ethylbenzene	0.11	7.1E-04	7.5E-11
Xylenes	0.61	7.3E-04	5.5E-11
Aromatics	1.8	7.1E-04	2.9E-12
Aliphatic C5-C8	32	7.2E-04	1.1E-07
Aliphatic C9-C12	4.7	7.1E-04	2.6E-06
SUM	40	-	-
Single Component Source			
Component	Vapor Source Concentration (mg/L-vapor)	Attenuation Factors	
		No Biodegradation	With Biodegradation
Benzene	40	7.3E-04	3.7E-11

Table 7—Predicted Attenuation Factors for NAPL Multiple-Component Source and Equivalent Single Component Source for Slab-on-Grade Scenario and Source Depth of 10 m bgs

NAPL Multiple-Component Source			
Weathered Gasoline Group/Component	Vapor Source Concentration (mg/L-vapor)	Attenuation Factors	
		No Biodegradation	With Biodegradation
Benzene	0.68	3.5E-04	1.6E-12
Toluene	4.0	3.5E-04	6.1E-12
Ethylbenzene	0.53	3.5E-04	7.6E-12
Xylenes	2.7	3.5E-04	5.6E-12
Aromatics	16	3.3E-04	2.8E-13
Aliphatic C5-C8	255	3.6E-04	1.3E-08
Aliphatic C9-C12	5.3	3.4E-04	3.5E-07
SUM	285	-	-
Single Component Source			
Component	Vapor Source Concentration (mg/L-vapor)	Attenuation Factors	
		No Biodegradation	With Biodegradation
Benzene	285	3.5E-04	1.9E-12

5. Evaluation of Additional Parameters

A few additional scenarios were simulated to evaluate the effect of soil type, foundation crack location and the presence of a high-moisture content soil layer.

5.1 Effect of Soil Type

The simulations presented above were performed using material properties corresponding to sandy soil. To assess the sensitivity of the model results to the geologic material properties, additional simulations were conducted assuming silty-clay soils. A comparison of the soil physical properties for the sand and silty-clay scenarios is shown in Table 8. Effective diffusion coefficients for the silty clay soils are approximately 3 times lower than those for sandy soils and the soil air permeability for silty clay is about two orders of magnitude lower than that for sandy soils.

Table 8—Soil Physical Properties (USEPA 2002)

Soil Type	Sand	Silty Clay
Soil bulk density (kg/m^3)	1660	1380
Soil air permeability (m^2)	1.0E-11	1.5E-13
Moisture filled porosity (v/v)	0.054	0.216
Total soil porosity (v/v)	0.375	0.481
Benzene effective diffusion coefficient (m^2/h)	5.12E-03	1.65E-03
Oxygen effective diffusion coefficient (m^2/h)	1.16E-02	3.74E-03

Simulations to assess the effect of soil type were performed assuming a basement foundation, a source depth of 5 m bgs, a first order biodegradation rate λ = 0.79 h^{-1}, and vapor source concentrations ranging from 0.4 to 200 mg/L-vapor. Additional simulations were performed using a vapor source concentration of 10 mg/L and a range of source depths from 3 to 7 m bgs (equivalent to 1 to 5 m below the foundation). With the exception of the soil properties, all other input parameters listed in Table 1 were used.

Normalized soil gas concentration distribution for sand and silty clay scenarios are presented in Figure 18. This figure indicates lower oxygen and hydrocarbon concentrations are predicted for silty clay soils. These trends are a result of increased biodegradation in the soils with the lower effective diffusion coefficient. Figures 19 and 20 show the variability in attenuation factors as a function of source concentration and source depth, respectively. The results show generally similar trends for both soil types although the bio-attenuation is much more significant for the silty clay soil. The difference between the attenuation factors for the cases with no degradation show the relative differences in attenuation attributable to physical processes alone (slower diffusion and advection through silty clay compared to sand). These results indicate that the attenuation factors calculated for sandy soils may be conservative indications of the effect of bio-attenuation for a range of soil conditions.

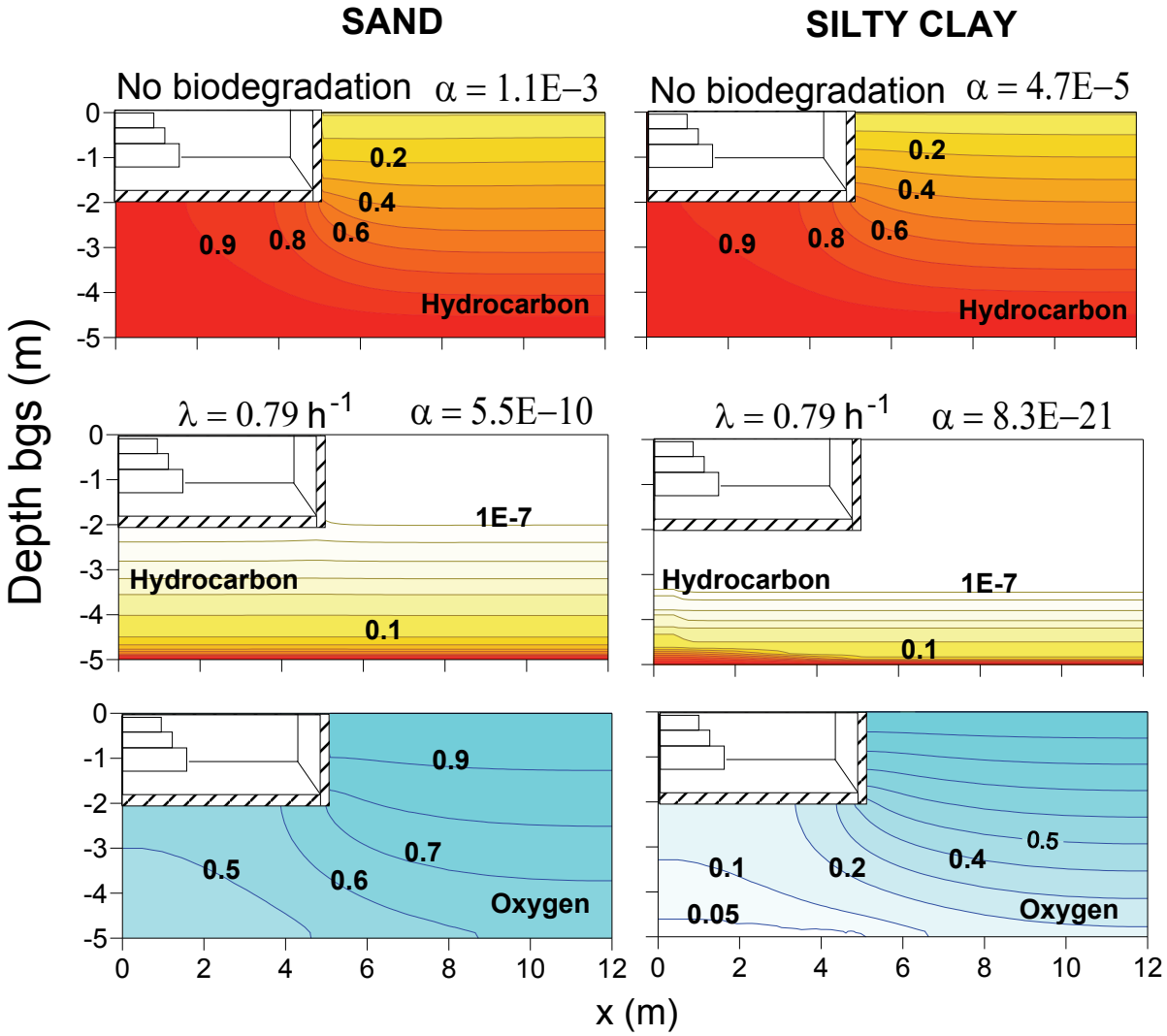

Figure 18—Normalized steady-state soil gas concentration distribution for oxygen and hydrocarbon with a vapor source concentration of 4 mg/L located at 5 m bgs (3 m below the foundation). The top hydrocarbon contour plots are for a no biodegradation case and the bottom hydrocarbon and oxygen contour plots are for a biodegradation case with first order rate λ = 0.79 h^{-1}. Hydrocarbon and oxygen concentrations are normalized by source and atmospheric concentrations, respectively. Qs (sand) = 3.7 L/min and Qs (silty clay) = 0.05 L/min.

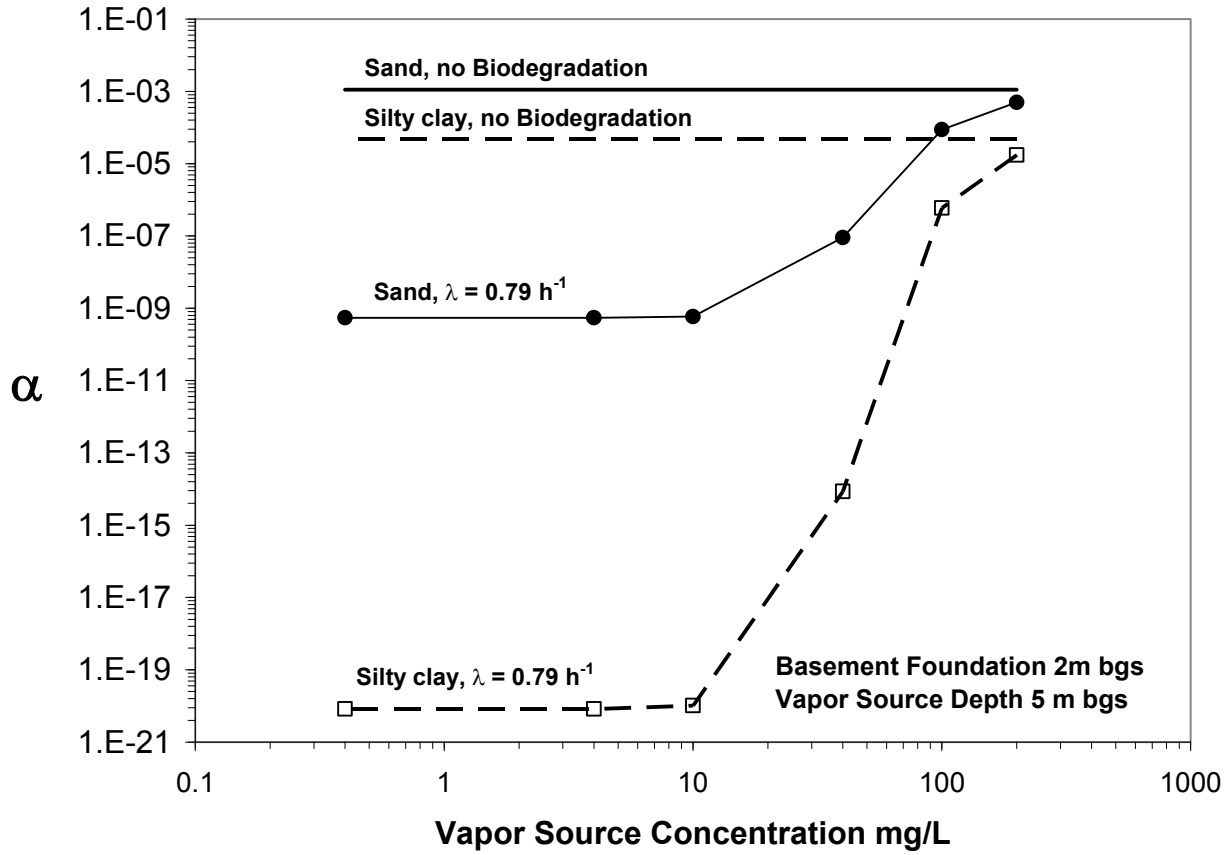

Figure 19—Attenuation factors as a function of soil type and vapor source concentration for a source located at 5 m bgs (3 m below a basement foundation). The graph present results for no biodegradation scenarios and biodegradation scenarios with a first-order biodegradation rate $\lambda = 0.79\ h^{-1}$. Qs (sand) = 3.7 L/min and Qs (silty clay) = 0.05 L/min.

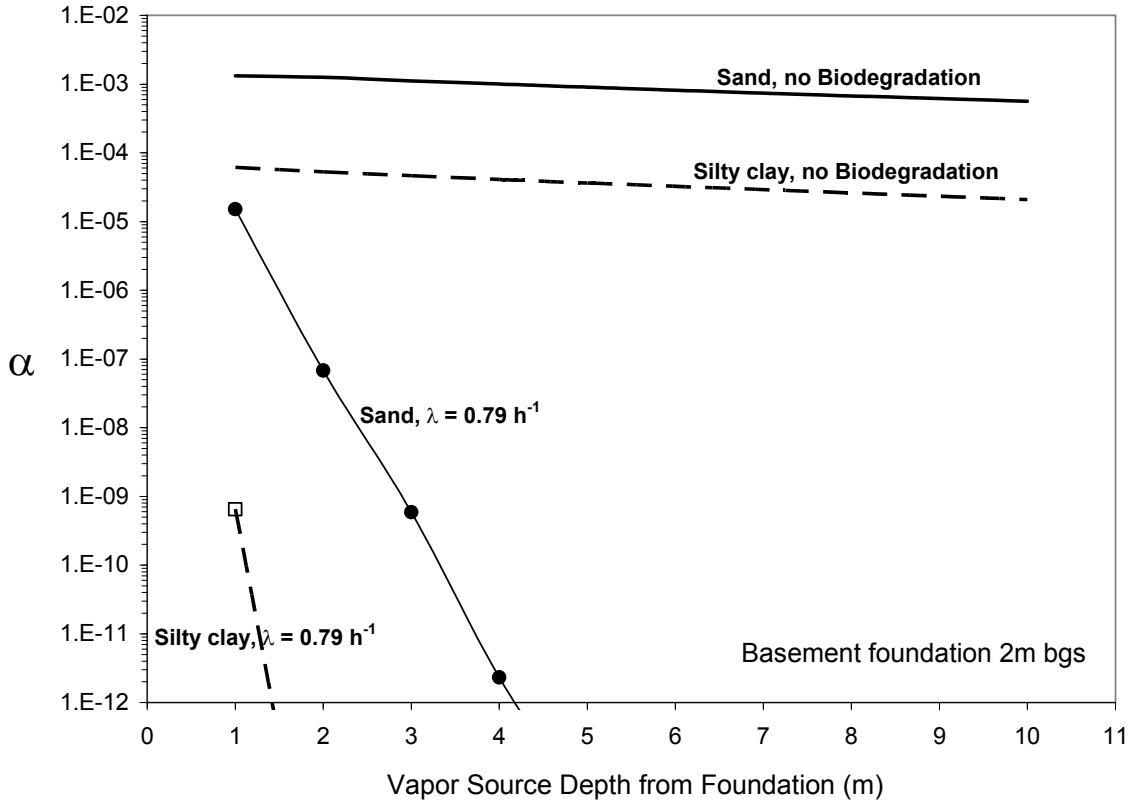

Figure 20—Attenuation factors as a function of soil type and source depth below a basement foundation for a 10 mg/L source vapor concentration. The graph presents results for no biodegradation scenarios and biodegradation scenarios with a first-order biodegradation rate $\lambda = 0.79\ h^{-1}$. This graph is applicable to all sources with vapor concentration ≤ 10 mg/L. Qs (sand) = 3.5 - 4 L/min and Qs (silty clay) = 0.05 – 0.06 L/min.

5.2 Effect of Foundation Crack Location

All simulations presented in the sections above assume a foundation crack located along the perimeter of the slab. The effect of crack location on the predicted attenuation factors previously evaluated by Abreu (2005) is summarized here (the effect on pressure-induced soil gas flow rate into the structure, Qs, is presented in Appendix A).

Figures 21 and 22 show the effect of crack location on α-values for a range of source concentration and source depth of 1 and 3 m below a foundation slab respectively. Figure 21 shows that the effect of crack location on α-values is not significant for sources with low vapor concentration (less than about 2 mg/L) at a shallow depth (1 m below a basement foundation). Figure 22 indicates that as the source-foundation separation increases there is an increase on the source concentration range over which the effect of crack location on α-values is not significant.

Based on these results, it is reasonable to estimate that α-values are primarily dependent on source depth and biodegradation rates and are not significantly dependent on crack location for scenarios with vapor source concentrations less than approximately 2 mg/L.

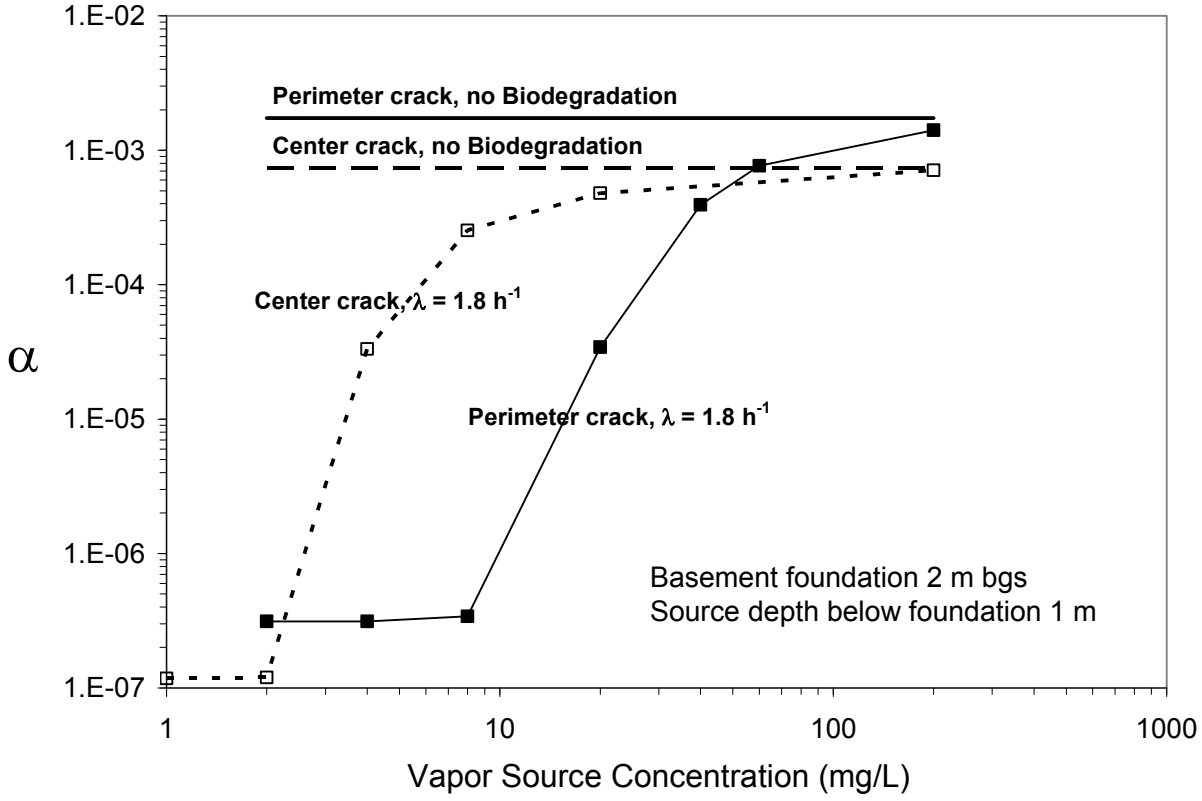

Figure 21—Effect of crack positioning (perimeter vs center of foundation) on attenuation factors as a function of vapor source concentration located 1 m below a basement foundation (Abreu, 2005).

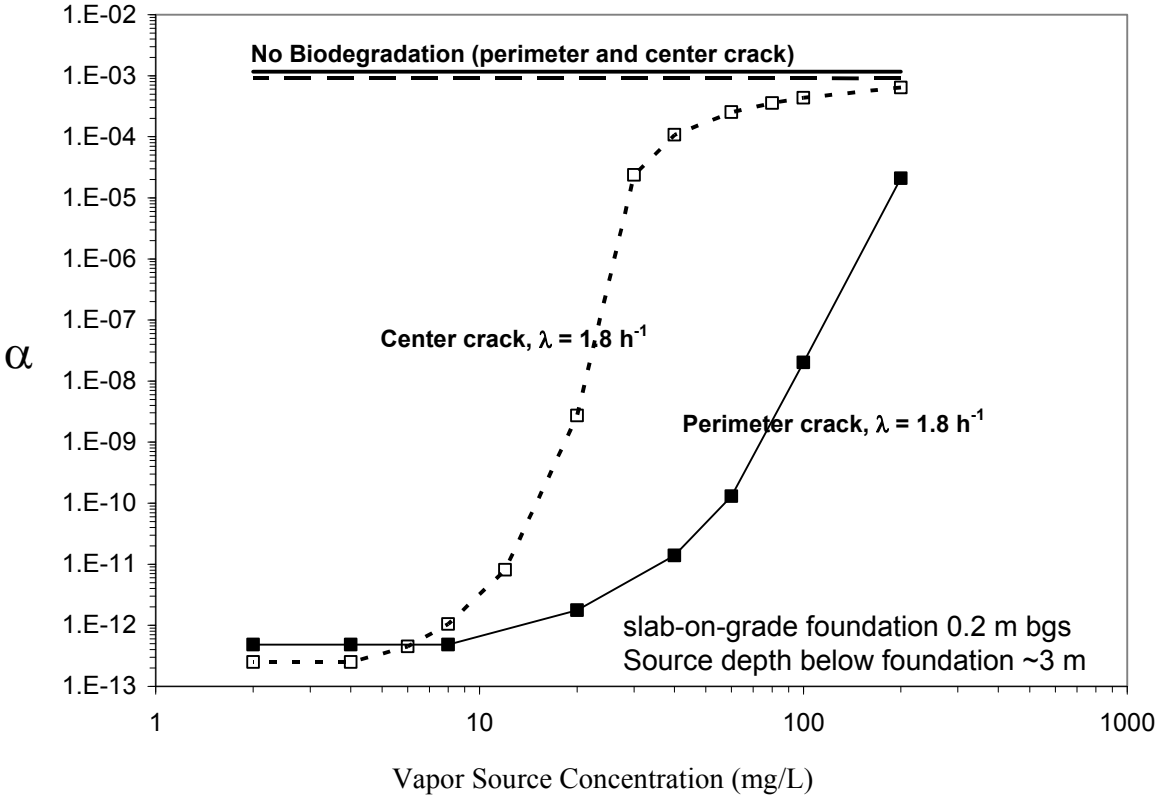

Figure 22—Effect of crack positioning (perimeter vs center of foundation) on attenuation factors as a function of vapor source concentration located 3 m below a slab-on-grade foundation (Abreu, 2005).

5.3 Effect of a High Moisture-Content Soil Layer

High moisture content in shallow soil may inhibit oxygen migration from the atmosphere to the subsurface porous media. Because aerobic biodegradation depends on the migration of oxygen downward from atmosphere, simulations were performed to assess the effect of a thin silty clay layer located at the ground surface on the oxygen transport downward from atmosphere. These simulations included a soil profile consisting of a 60-cm silty clay soil layer at the ground surface overlying a homogeneous sandy soil layer. Simulations were run for basement scenarios with vapor source concentrations of 1 and 10 mg/L at a depth of 4 m bgs (2 m below foundation). The results are presented in Figures 23 and 24. The concentration profile and attenuation factor presented in Figure 23 shows that the thin silty clay layer has no effect in reducing biodegradation for a 1 mg/L vapor source. However, Figure 24 shows that for the scenario of a 10 mg/L vapor source at a depth of 2 m below foundation, the reduced oxygen flux from the surface due to the silty clay layer results in an oxygen deficient zone in the subsurface and a higher attenuation factor. Nevertheless, this reduced biodegradation effect is expected to decrease as the source depth increases.

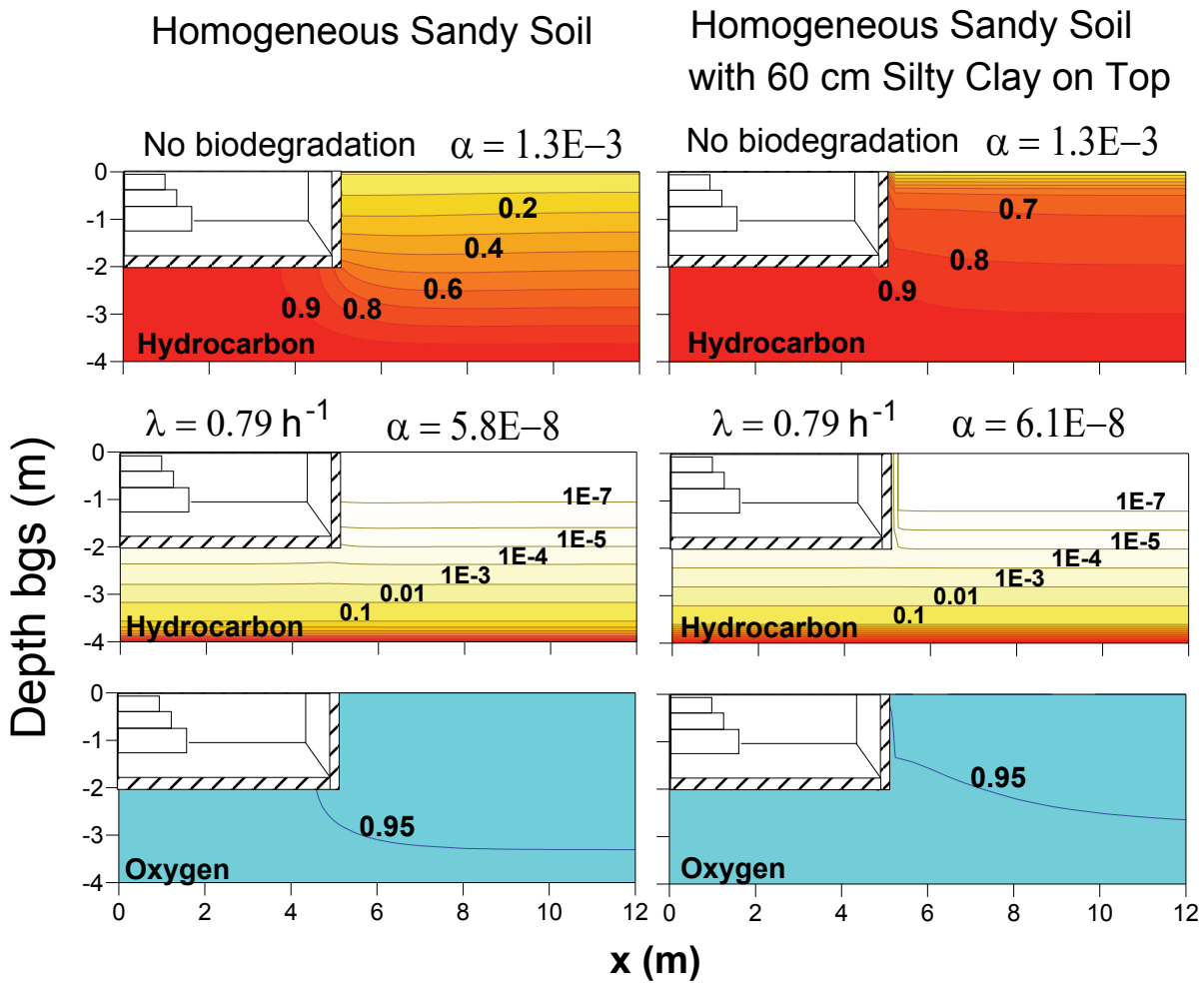

Figure 23—Normalized steady-state soil gas concentration distribution for oxygen and hydrocarbon with a vapor source concentration of 1 mg/L located at 4 m bgs (2 m below a basement foundation). Two soil lithology are illustrated: Homogeneous and layered. The top hydrocarbon contour plots are for a no biodegradation case and the bottom hydrocarbon and oxygen contour plots are for a biodegradation case with first order rate $\lambda = 0.79\ h^{-1}$. Hydrocarbon and oxygen contours are normalized to source and atmospheric concentrations, respectively.

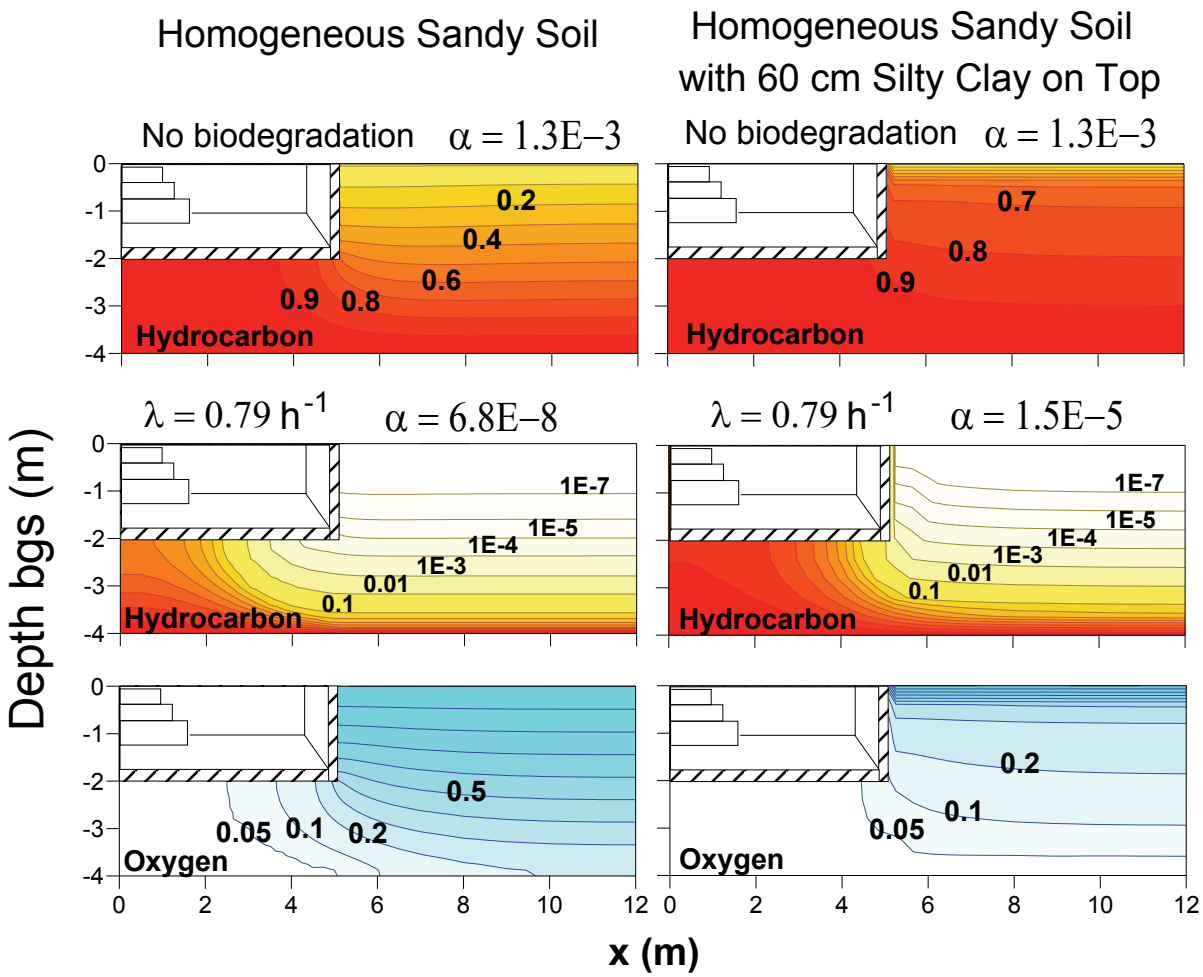

Figure 24—Normalized steady-state soil gas concentration distribution for oxygen and hydrocarbon with a vapor source concentration of 10 mg/L located at 4 m bgs (2 m below a basement foundation). Two soil lithology are illustrated: Homogeneous and layered. The top hydrocarbon contour plots are for a no biodegradation case and the bottom hydrocarbon and oxygen contour plots are for a biodegradation case with first order rate $\lambda = 0.79\ h^{-1}$. Hydrocarbon and oxygen contours are normalized to source and atmospheric concentrations, respectively.

6. Discussion

The findings of this study may be useful for vapor intrusion assessments at petroleum hydrocarbon sites. Consideration of vadose-zone biodegradation of petroleum hydrocarbons should be incorporated in the development of a site conceptual model and site-specific assessment planning.

6.1 Development of a Conceptual Model

A conceptual model of the fate and transport of chemicals should form the foundation for any assessment of the potential health risks. Conceptual models are developed using available site-specific information, theoretical knowledge of physical, chemical and biological processes, and mechanisms affecting fate and transport and experience gained from other sites with similar chemicals and geologic conditions. The simulations presented in this paper should help with developing a conceptual model for the fate and transport of degradable vapors because they show the theoretical implications for a very wide variety of common site conditions.

Results of this study suggest several key factors to consider in the conceptual model for biodegradable compounds:

- Source concentration: Attenuation factors are independent of source concentration for source concentrations less than about 10 mg/L-vapor for the scenarios evaluated in this study assuming perimeter crack location. If the source concentration is below this level, use of the low source concentration attenuation factors predicted in Figures 12 and 13 should be appropriate. However, for vapor source concentrations above this level, the attenuation factor is dependent on source concentration and the results presented in Appendices B and C should be considered.

- Biodegradation rate: Vadose zone aerobic biodegradation can have a significant impact on vapor intrusion attenuation factors. The results presented in this study indicate that predicted attenuation factors, assuming average biodegradation rates, may be several orders of magnitude smaller than the no-biodegradation estimates.

- Soil physical properties (e.g. moisture content and porosity): Lower effective diffusion coefficients in soil will be present in higher moisture content soils. The effect of biodegradation is greater in soils with higher moisture content and lower effective diffusion coefficients. Therefore the attenuation factors predicted in this study, which assumed soil properties for sandy soils should provide reasonably conservative α-values estimates for relatively homogeneous soils.

- Depth to source: Attenuation factors decrease with increasing depth to source. For cases with a site conceptual model similar to those considered in this study, a vapor source total hydrocarbon concentration less than about 1 mg/L, a foundation-source separation of approximately 1 m is likely sufficient to result in insignificant risks due to the vapor intrusion pathway. For high source concentration scenarios (e.g. >100 mg/L-vapor), a foundation-source separation of approximately 10 m is likely be sufficient to result in insignificant risks due to the vapor intrusion pathway.

6.2 Preliminary Screening

The simulations presented in this paper indicate that sites with petroleum hydrocarbon sources that are either deep or have low concentrations are unlikely to pose a risk via the vapor intrusion pathway because degradation will reduce the vapor concentrations in the subsurface prior to entry to overlying buildings. The attenuation factors presented in this study can be used to estimate site-specific soil vapor screening levels for biodegradable compounds, providing there is sufficient site-specific information available to characterize the source depth, source concentration and presence of oxygenated conditions, and verify that the geologic and building conditions are similar to those simulated herein. This is analogous to selecting a semi site-specific attenuation factor for non-degradable compounds presented in the draft OSWER Guidance on vapor intrusion (EPA, 2002).

Multiplying an appropriate attenuation factor by a measured vapor source concentration will yield a preliminary estimate of potential indoor air concentrations, which can be compared to risk-based target levels. If groundwater concentrations are available, a conservative estimate of the vapor source concentration can be calculated by multiplying the groundwater concentration by the Henry's Law coefficient. Note, however, that the calculations presented in this study are based on vapor concentrations measured above the capillary fringe. Therefore, if groundwater data is used to estimate a source vapor concentration in this way, recognize that this approach does not account for potential additional attenuation due to rate-limiting transport or degradation across the capillary fringe. Also, the effect of mixing within conventional monitoring wells that can result in borehole dilution is not considered. Consequently, the use of groundwater concentrations times Henry's Law coefficient could either overestimate or underestimate the vapor source concentration.

If the calculated indoor air concentration is greater than the risk based screening level, further assessment is warranted. Where the calculated indoor air concentration is lower than the target indoor air concentration, the justification for additional assessment diminishes. The need for a preliminary assessment is generally a matter of regulatory policy and negotiation that will depend on a variety of factors. However, if the calculated indoor air concentrations are more than one order of magnitude lower than the target indoor air concentrations, the site or building may be a candidate for no further action.

6.3 Site-Specific Assessments

The findings of this study also may help in the design of an investigation program. Where bio-attenuation occurs, there are dramatic decreases in hydrocarbon concentrations over very narrow ranges of depth; therefore, vertical profiles of hydrocarbon vapor and oxygen concentrations can provide valuable information at many hydrocarbon sites. Deeper soil gas samples may be preferable for initial screening. If this approach is followed and total hydrocarbon vapor concentrations are less than about 2 mg/L and oxygen is present at concentrations above 1 %, it is likely that biodegradation will reduce concentrations below levels of concern and vapor intrusion may not result in unacceptable risks.

Additionally, soil gas concentration profile data may be used to evaluate the biodegradation rate at sites which could be used to estimate an attenuation factor considering biodegradation (Johnson, et al. 1999, Ettinger and McAlary, 2005). However, it may be difficult to experimentally determine biodegradation rates under field conditions, because vadose zone biodegradation may result in many orders of magnitude reduction in hydrocarbon soil gas concentrations to levels below detection limits. Nevertheless, field measurements may be used to estimate a lower bound for the biodegradation rate constant for a site-specific evaluation.

6.3.1 Example Application

This section provides a practical example to demonstrate how this research could be applied for screening sites with moderate to low hydrocarbon concentrations to assess the potential for vapor intrusion. The example considers a residential structure with a 2 m deep basement located above groundwater containing dissolved hydrocarbons with a 4 m thick vadose zone comprised of homogeneous sandy soil. The concentration of TPH in groundwater is 3 mg/L. Assuming equilibrium phase partitioning between groundwater and deep soil gas according the Henry's Law, the TPH concentration in deep soil gas would be about 10 mg/L.[1]

The following steps would be appropriate for assessing the potential for vapor intrusion:

Step	Activities	Example Application
1) Conceptualize	Collect data to verify that site conditions reasonably match model scenarios. Use theory and experience to assess whether model is relevant and proceed only if it is, or with a reasonable degree of caution and data collection to compensate for differences between model scenario(s) and site conditions.	The example scenario was developed to be consistent with model formulation, but in general this assumption should not take this for granted.
2) Identify site-specific inputs.	Collect data to establish vapor source concentrations, depth, geologic conditions, and building type.	The site specific inputs considered in this evaluation are: Source concentration: 10,000 μg/L. Concentrations of individual constituents are listed in Table 9. Building construction: Basement Depth to groundwater: 4 m Degradation rate constant: 0.79 hr^{1} assumed.
3) Look-up Attenuation Factor	Refer to Table 4 or 5 and select the appropriate attenuation factor. The TPH source vapor concentration should be used in this evaluation (not the concentration of an individual constituent, unless it is a single component source).	For this example an α-factor of about 1E-7 is supported.

[1] The soil gas TPH concentration is calculated by summing the calculated soil gas concentrations for each fraction (i.e. $C_{VS} = \sum C_{GW,i} \times H_i$ where C_{VS} is the soil gas TPH concentration, $C_{GW,i}$ is the groundwater concentration for fraction i, and H_i is the Henry's law coefficient for fraction i).

4) Calculate indoor air concentrations for individual constituents	Multiply the source vapor concentrations by the site-specific attenuation factor identified in the previous step.	Results are presented in Table 9.
5) Assess Potential Risks	Compare the predicted indoor air concentrations to target risk-based indoor air concentrations or calculate risks using the predicted indoor air concentrations, and consider uncertainty. If risks are unacceptable or marginal, consider additional data collection (vertical soil gas profiles, sub-slab or indoor air sampling) or pre-emptive mitigation.	In this example, risk-based concentrations from the Draft OSWER Vapor Intrusion Guidance (EPA, 2002) (assuming 1E-06 target risk level for carcinogens) are used. The predicted indoor air concentrations for the individual constituents are below risk-based target levels.
6) Ground-truth with data	Using a conceptualization of the site conditions informed by expectations from these model results, collect necessary and sufficient data to verify site conditions	Verify data is sufficient to support decision-making and conceptual model.

As shown in Figure 12, the vapor intrusion attenuation factor assuming the average degradation rate constant (λ = 0.79 hr^{-1}) for the case with the source located 2 m below the foundation is 1E-07. The vapor source concentrations for the individual constituents are taken from the speciation presented in Section 4.5. The predicted indoor air concentration and comparison to risk-based levels is shown in Table 9.

Table 9—Example Calculations

Compound	Source groundwater concentration (mg/L)	Henry's Law Coefficient (cm^3/cm^3)	Source vapor concentration (mg/L)	Predicted IA (ug/m^3)	Target IA (ug/m^3)
Benzene	0.05	0.23	0.01	0.001	0.31
Toluene	0.4	0.27	0.1	0.01	400
Ethylbenzene	0.1	0.32	0.03	0.003	2.2
Xylene	0.5	0.30	0.15	0.015	7,000

For the conditions described in this example, the predicted indoor air concentrations are more than two orders of magnitude lower than the target indoor air concentrations, which indicate the risk via vapor intrusion would be negligible, providing there are no barriers to entry for atmospheric oxygen to the subsurface. Verification with appropriate data collection is nevertheless an important consideration, but this screening level assessment would indicate that risks are unlikely to be significant.

Although real sites may have additional complexities (geologic heterogeneity, non-steady flow conditions, different building characteristics, complex contaminant source distribution, etc.), the model simulations may still be used to provide a more relevant and reasonable initial screening criteria for degradable compounds than historic approaches that either assume there is no degradation or apply a single factor to account for the amount of attenuation caused by biodegradation. At a minimum, the conceptualization of the site conditions and selection of an approach for investigation and remediation should benefit from consideration of the theoretical analysis provided by the mathematical model.

7. Conclusions and Recommendations

7.1 Conclusions

- Provided that oxygen is present, aerobic biodegradation of petroleum hydrocarbon vapors in the unsaturated zone will reduce soil vapor concentrations and the potential risks from vapor intrusion to indoor air compared to non-degrading compounds. The magnitude of the reduction depends on site-specific conditions, especially the source concentrations, source depth, oxygen distribution and degradation rates, which should be considered in the development of a conceptual site model for

each site. The simulations presented here should help to formulate conceptual models for a variety of sites, and help with screening, prioritization and selection of data collection strategies for vapor intrusion assessments at petroleum release sites.

- Simulations presented in this paper represent a wide range of conditions that may be encountered at sites where vapor intrusion assessments are required due to groundwater impacted by petroleum. The predicted α-values presented here may produce more appropriate initial screening values than generic attenuation factors derived from data for non-degrading compounds, providing site conditions reasonably match the scenarios simulated.

- Oxygen supply and degradation rates are likely to be sufficient to mitigate potential risks from vapor intrusion for low vapor concentration sources (less than about 2 mg/L total hydrocarbons). Vapor intrusion at sites with higher source concentrations may also be mitigated to some degree depending on site-specific conditions, particularly the source-building separation distance. There appears to be a theoretical source-building separation distance beyond which degradation will mitigate vapor intrusion risks regardless of how high the source concentration is, although this distance may vary with site-specific conditions.

7.2 Recommendations

- Bio-attenuation should be incorporated in regulatory guidance documents, which would allow regulators and responsible parties to focus on sites with higher probability of vapor intrusion concerns.

- Regulators and practitioners should use the theoretical information presented in this and previous studies (Abreu and Johnson, 2006) to help interpret field data and select appropriate data collection strategies.

- Investigative approaches for assessing vapor intrusion should be different for biodegradable compounds compared to non-degrading chemicals. In assessing contaminant transport and biodegradation in the subsurface, measurement of the vapor source total hydrocarbon concentration and oxygen profile in the subsurface may be useful.

- Field data should be used to verify the model simulations, and as more studies are conducted, it may be appropriate to further update and revise the regulatory screening process for assessing vapor intrusion at hydrocarbon release sites.

8. References

Abreu, L. D. V. A Transient Three-Dimensional Numerical Model to Simulate Vapor Intrusion into Buildings. UMI 3166060; Ph.D. Dissertation, Arizona State University, Tempe, AZ, 2005.

Abreu, L. D. V.; Johnson, P. C. “Simulating the Effect of Aerobic Biodegradation on Soil Vapor Intrusion into Buildings: Influence of Degradation Rate, Source Concentration, and Depth,” *Environmental Science and Technology* 2006, 40 (7); 2304-2315.

Abreu, L. D. V.; Johnson, P. C. “Effect of Vapor Source-Building Separation and Building Construction on Soil Vapor Intrusion as Studied with a Three-Dimensional Numerical Model,” *Environmental Science and Technology* 2005, 39 (12), 4550-4561.

Bordon, R. C.; Bedient, P. B. Transport of dissolved hydrocarbons influenced by oxygen-limited biodegradation, 1. Theoretical development. *Water Resource Research* 1986, 22 (13), 1973-1982.

DeVaull, G. E. “Indoor Vapor Intrusion with Oxygen-Limited Biodegradation for a Subsurface Gasoline Source,” *Environmental Science and Technology* 2007, 41 (9), 3241-3248.

Ettinger, R.A. and T. McAlary. Site-Specific Vapor Intrusion Evaluation Including Biodegradation. Battelle In-Situ and On-Site Bioremediation Symposium, Baltimore, Maryland. June 6 – 9, 2005.

Johnson, P. C.; Stanley, C. C.; Kemblowski, M. W.; Byers, D. L.; Colthart, J. D. A Practical Approach to the Design, Operation, and Monitoring of In Sity Soil-Venting Systems. *Ground Water Monitoring and Remediation* 1990, May-June, 28 (3), 159-178.

Johnson, P.C., Mariush W. Kemblowski, and Richard L. Johnson. Assessing the Significance of Subsurface Contaminant Vapor Migration to Enclosed Spaces: Site-Specific Alternatives to Generic Estimates. Journal of Soil Contamination, 1999 8(3):389-421.

Roggemans, S.; Bruce, C. L.; Johnson, P. C. "Vadose Zone Natural Attenuation of Hydrocarbon Vapors: An Empirical Assessment of Soil Gas Vertical Profile Data," API Technical Bulletin No. 15. American Petroleum Institute, Washington, DC, 2001.

TPHCWG. Selection of Representative TPH Fractions Based on Fate and Transport Considerations. Total Petroleum Hydrocarbon Criteria Working Group Series. Amherst Scientific Publishers, Amherst, MA, volume 3, 1997.

USEPA. Soil Screening Guidance: User's Guide, Second Edition. Office of Solid Waste and Emergency Response, Publication 9355.4-23, July 1996.

Appendix A

Predicted Soil Gas Pressure Field and Air Flow Rate into the Building

Introduction

This appendix provides information on the advective component of soil gas transport for the simulations conducted in this study.

Predicted Soil Gas Pressure Field and Air Flow Rate into the Building

Examples of the normalized pressure fields for both the basement and slab-on-grade scenarios as well as the calculated pressure-induced soil gas flow rates (Qs) for soil conditions studied is this work are presented in Figure A1. The Figure includes profiles where the water table (lower model boundary) is located at depths of 3 m, 5 m, and 7 m below ground surface (bgs). Each profile is specific to the case where the soil properties are homogeneous (K_g=10^{-11} m^2), the building is under-pressurized by 5 Pa and 0.001-m wide foundation cracks are located along the perimeter of the foundation. Figure A1 shows that the disturbance pressure field and the resulting flow field are qualitatively similar for the basement and slab-on-grade constructions. In brief, the pressure fields suggest air flow primarily traveling down from ground surface and then to the foundation crack located along the perimenter of the foundation slab, with flow beneath the foundation becoming more pronounced as the depth to groundwater (lower boundary) increases. The pressure-induced soil gas flow rates from the subsurface and into the buildings predicted for sandy soil type, range from about 3 to 5 L/min, with flow rates generally being larger for slab-on-grade constructions and deeper depths to groundwater.

Predicted Effect of Crack Location on Soil Gas Pressure Field and Air Flow Rate into the Building

Abreu (2005) studied the effect of crack location on the pressure field in the subsurface and the resultant air flow rate into the building. The crack configurations used in her work are presented in Figure A2.

Figures A3 and A4 present the disturbance pressure fields for basement and slab-on-grade foundation scenarios. The soil properties are homogeneous (K_g=10^{-11} m^2), the building is under-pressurized by 5 Pa and 0.001-m wide foundation cracks are located either along the perimeter or at the center of the foundation. In the case of the perimeter crack, the flow path is iqual to the one presented in Figure A1 and discussed above. For the center-of-foundation crack scenarios, the flow is primarily horizontal beneath the foundation, and the uniformity of the flow increases as the depth to groundwater decreases. Figure A5 shows predicted Qs as a function of foundation type (basement vs. slab-on-grade), crack positioning (perimeter and center of foundation slab) and water table depth below grade surface for a constant building under-pressurization of 5 Pa. Figures A3, A4 and A5 shows that the difference in Qs predictions between similar perimeter crack and center-of-foundation crack scenarios differs on average by a factor of 2, with the flows to the perimeter crack being greater. The flow to a perimeter crack is expected to be larger than the flow to a center-of-foundation crack because of the shorter flow path length from ground surface to a perimeter crack.

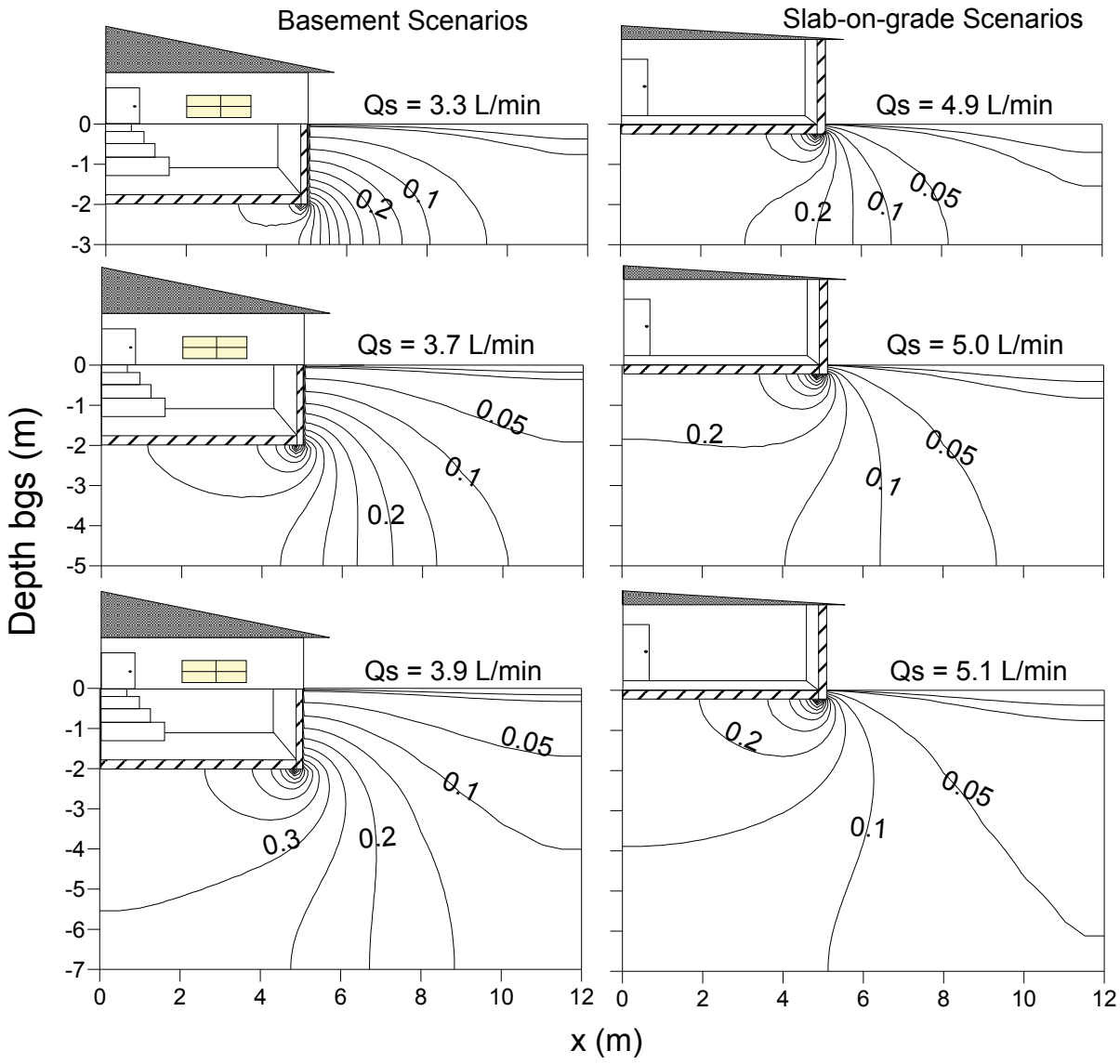

Figure A1—Normalized steady-state disturbance pressure distribution for a homogeneous soil permeability field (K_g=10^{-11} m^2) surrounding basement and slab-on-grade foundations with perimeter cracks and a lower boundary at depths of 3, 5 and 7 m bgs. The contours of constant disturbance pressure are normalized to the disturbance pressure in the building (5 Pa under-pressurization) and the predicted airflow rate into the building (Qs) is indicated for each scenario.

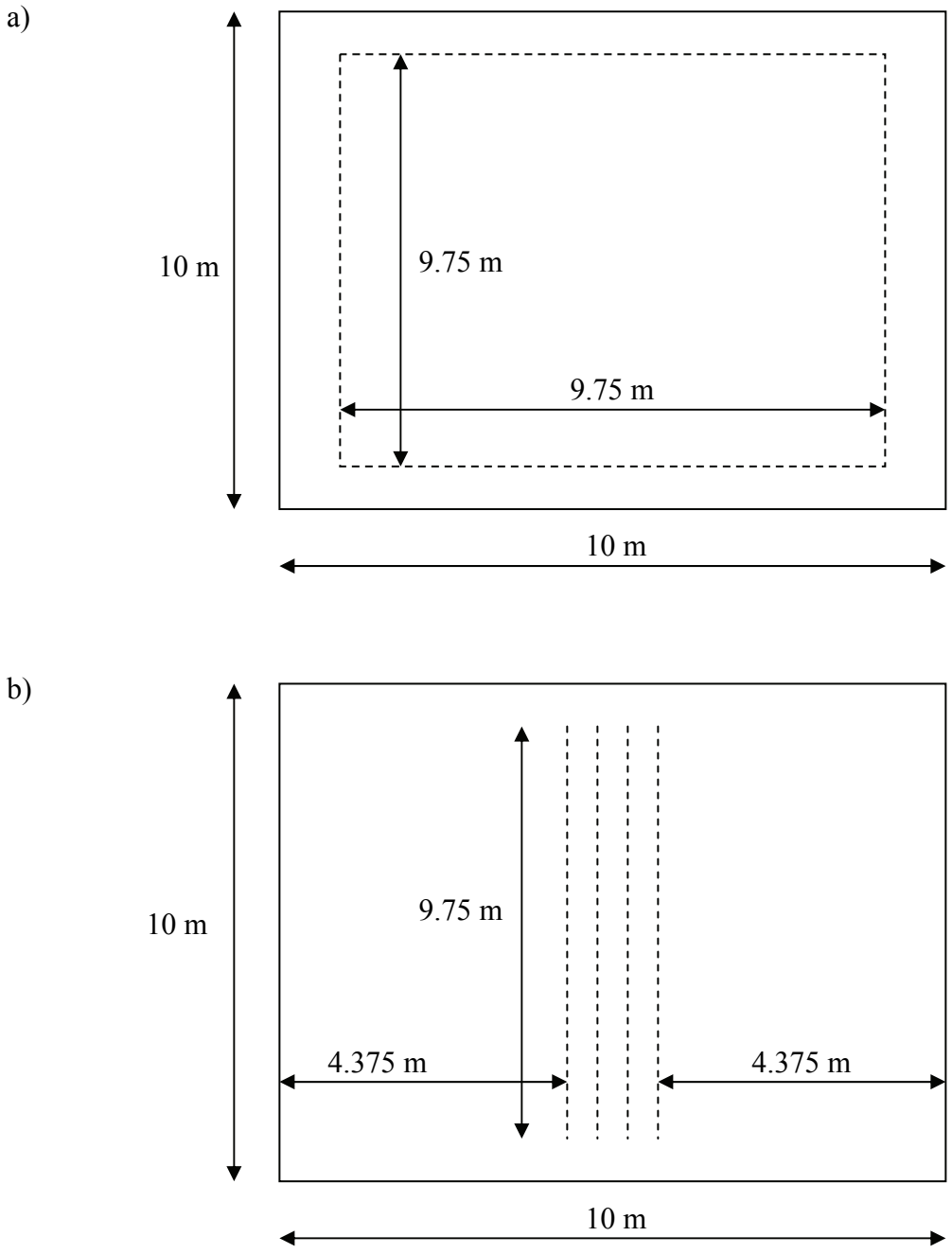

Figure A2—Plan view of the foundation crack distribution (dashed lines): a) perimeter crack; b) center-of-foundation cracks.

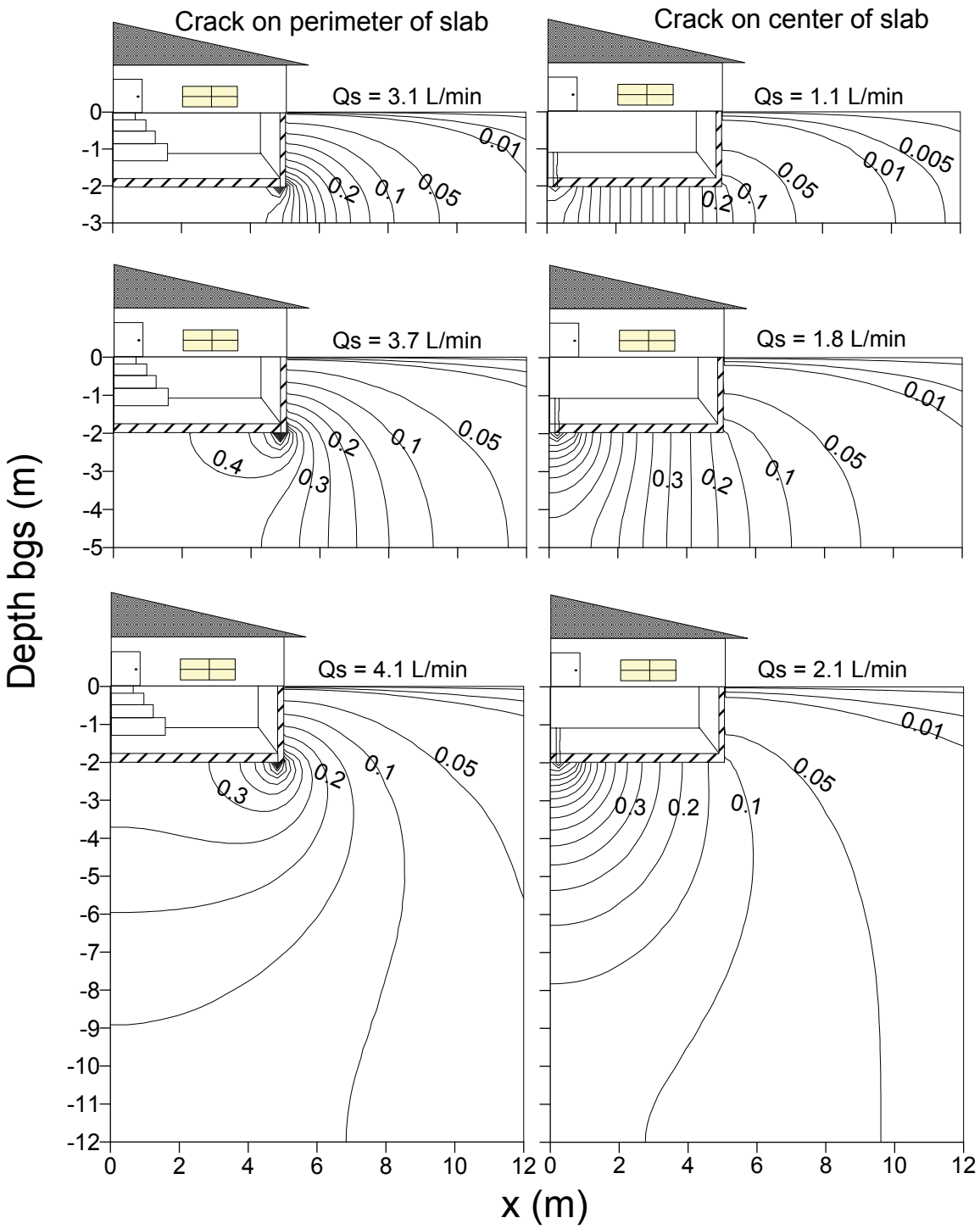

Figure A3—Normalized steady-state disturbance pressure distribution for a homogeneous soil permeability field (K_g=10^{-11} m^2) surrounding basement foundations with cracks located on perimeter and on center of the foundation slab. The scenarios present lower boundary (ground water level) at depths of 3, 5 and 12 m bgs. The contours of constant disturbance pressure are normalized to the disturbance pressure in the building (5 Pa) and the predicted airflow rate into the building (Qs) is indicated for each scenario (Abreu, 2005).

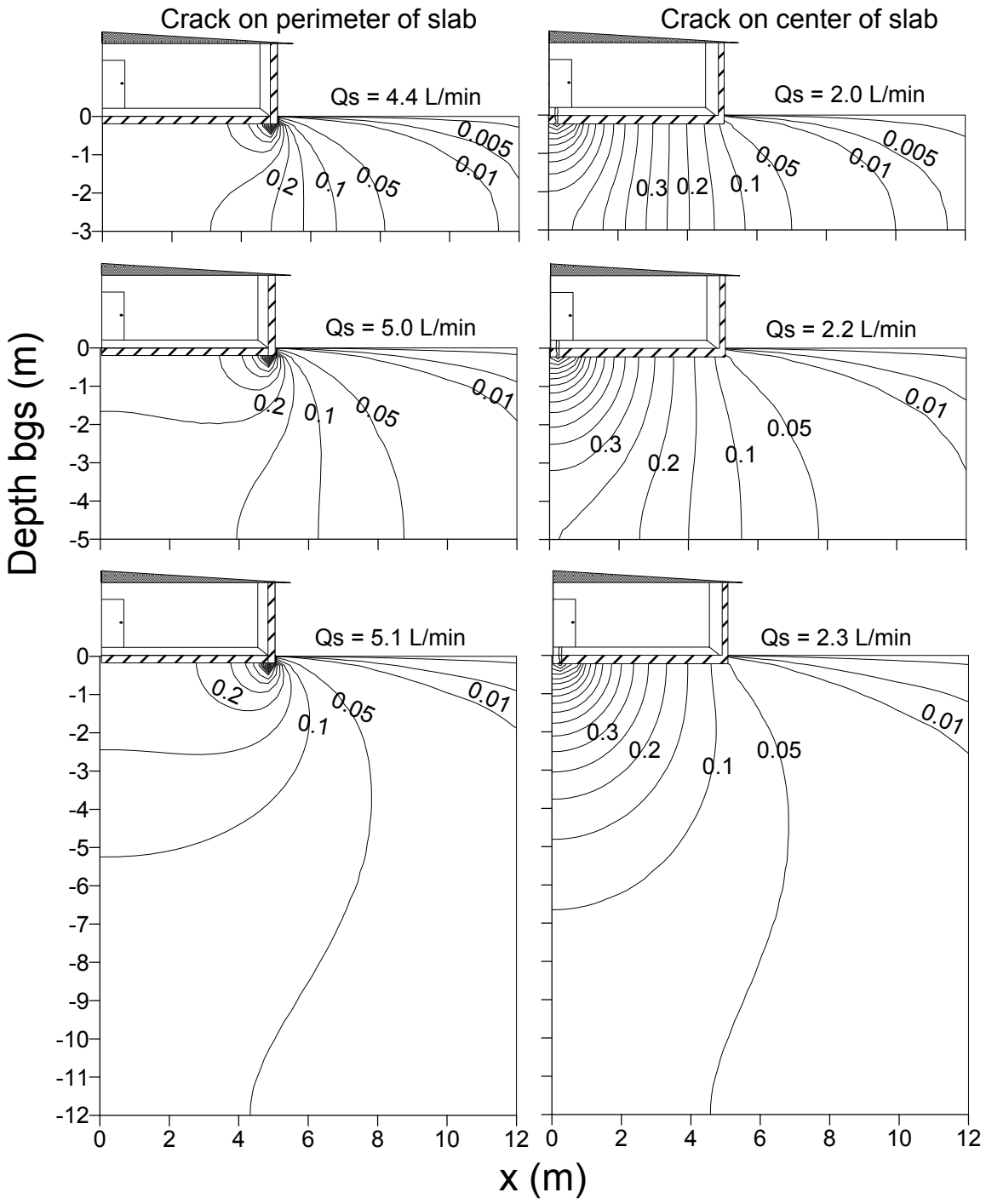

Figure A4—Normalized steady-state disturbance pressure distribution for a homogeneous soil permeability field (K_g=10^{-11} m^2) below slab-on-grade foundations with cracks located on perimeter and on center of the foundation slab. The scenarios present lower boundary (ground water level) at depths of 3, 5 and 12 m bgs. The contours of constant disturbance pressure are normalized to the disturbance pressure in the building (5 Pa) and the predicted airflow rate into the building (Qs) is indicated for each scenario (Abreu, 2005).

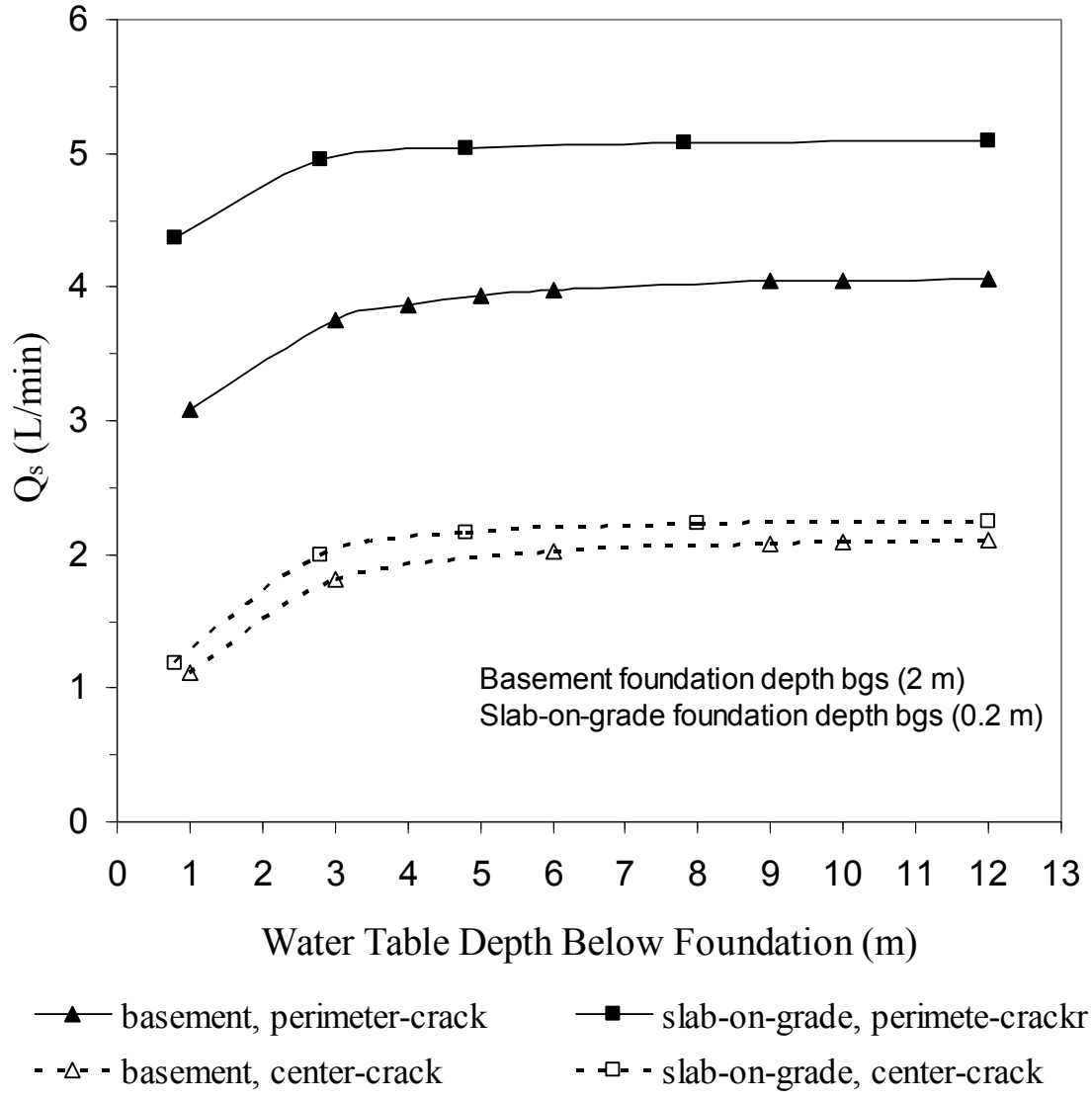

Figure A5—Effect of crack positioning (perimeter vs center of foundation) on soil gas flow (Qs) into the building for basement and slab-on-grade structures under-pressurized by 5 Pa and sand soil subsurface with air permeability of 1E-11 m^2 (Abreu, 2005).

Appendix B

Plots of Attenuation Factors as a Function of Source Concentration, Depth and First-order Biodegradation Rates for Basement Scenarios

Introduction

This appendix summarizes the attenuation factors predicted in this work for basement scenarios on homogeneous sandy soils, building constant under-pressurization of 5 Pa and full-perimeter cracks. The α-values are presented as a function of source-foundation separation for a vapor source concentration of 10 mg/L (this graph is application to all vapor source concentrations that smaller than 10 mg/L) and α-values are presented as a function of vapor source concentration for several source depths (D) and equivalent source-foundation separation (L). All graphs present α-values for three biodegradation rates (λ) and for the no-biodegradation case for comparison purposes.

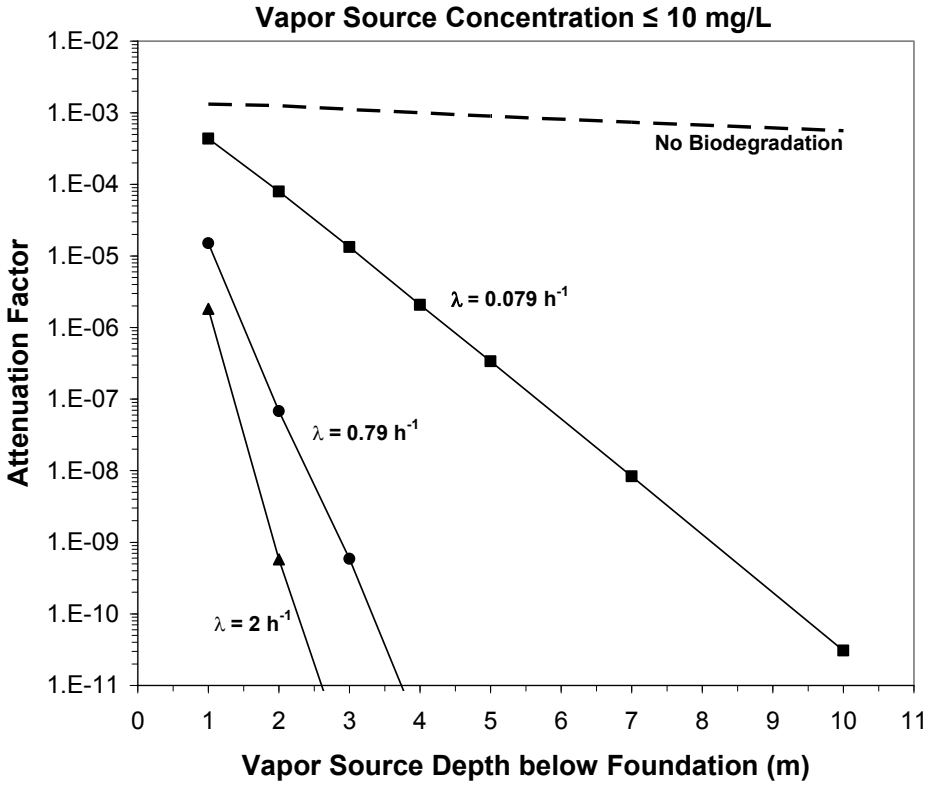

D = Source depth below ground surface
L = source foundation separation

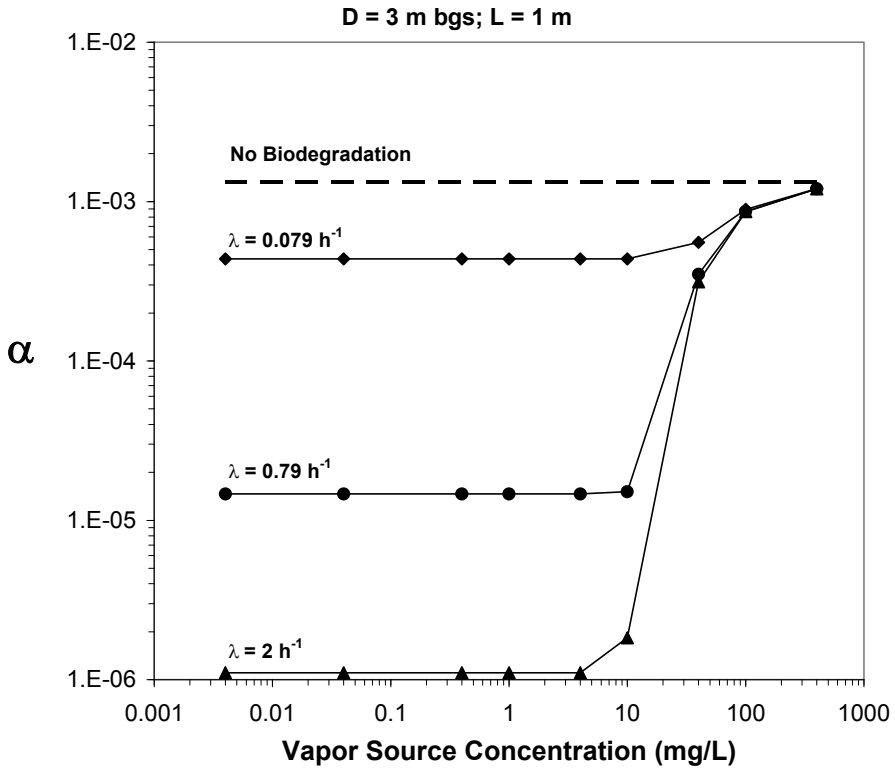

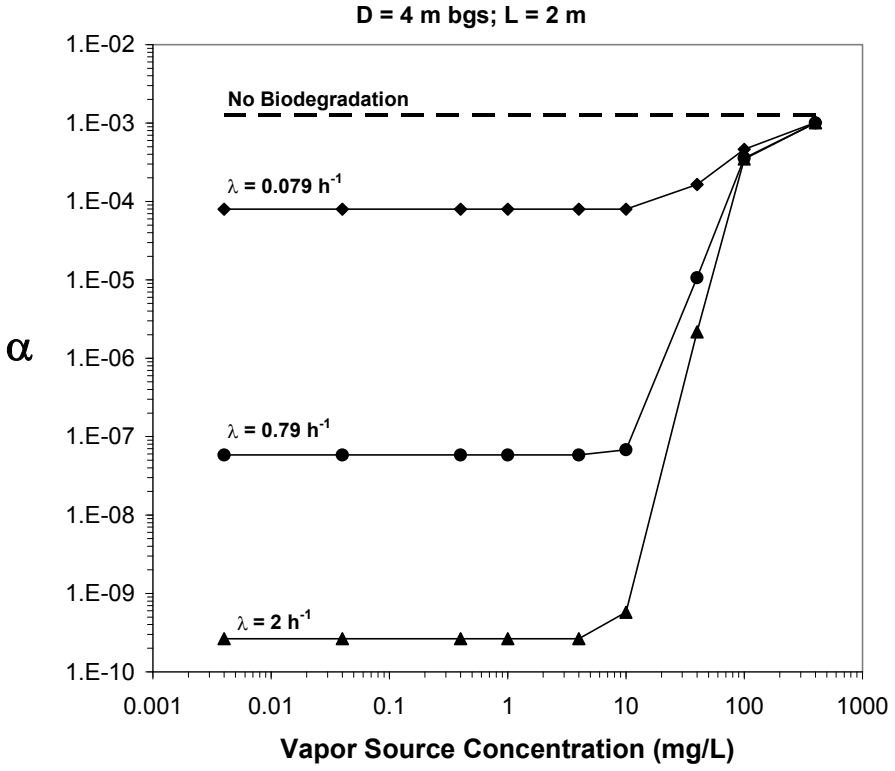

D = Source depth below ground surface
L = source foundation separation

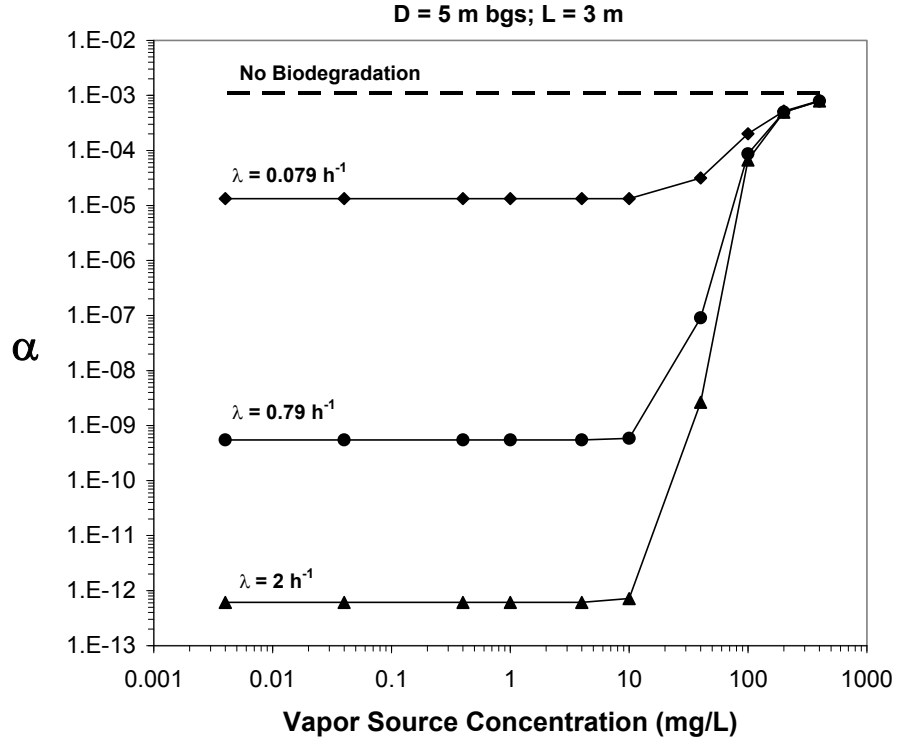

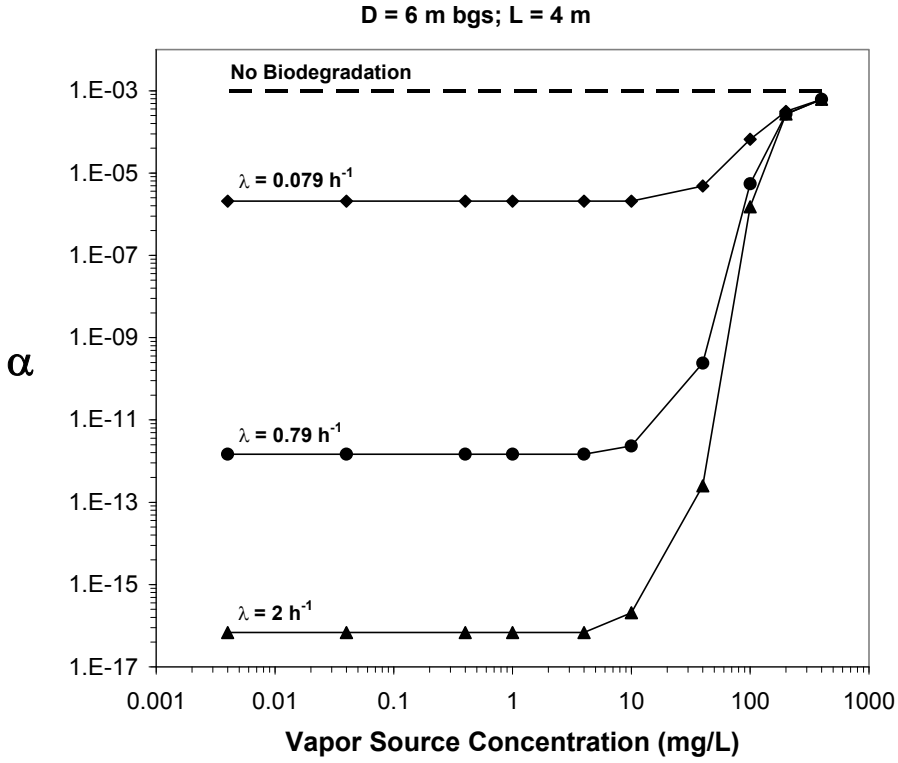

D = Source depth below ground surface
L = source foundation separation

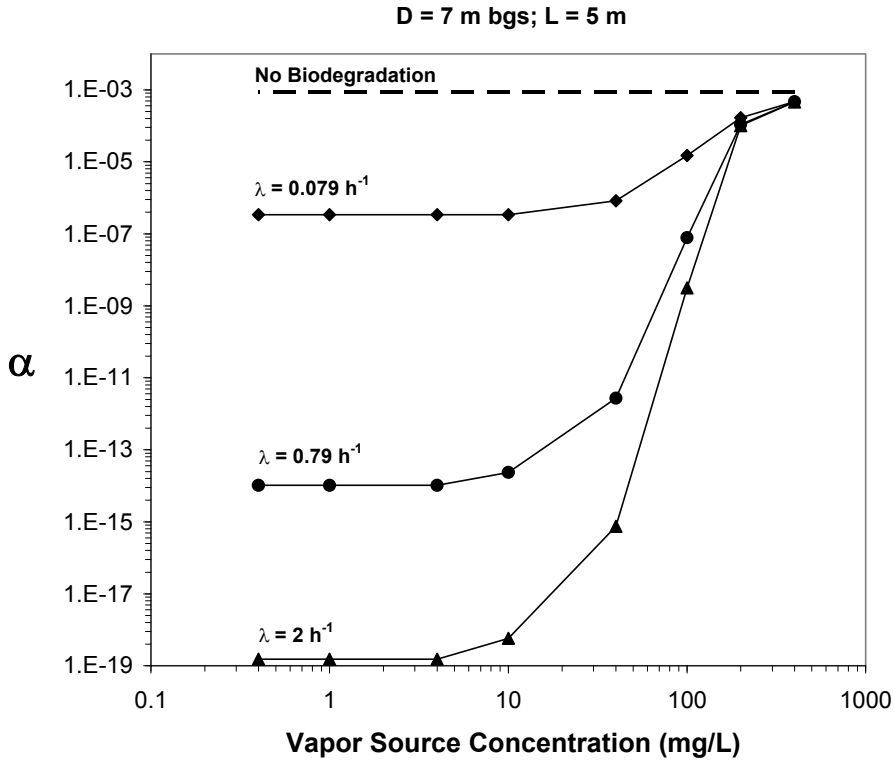

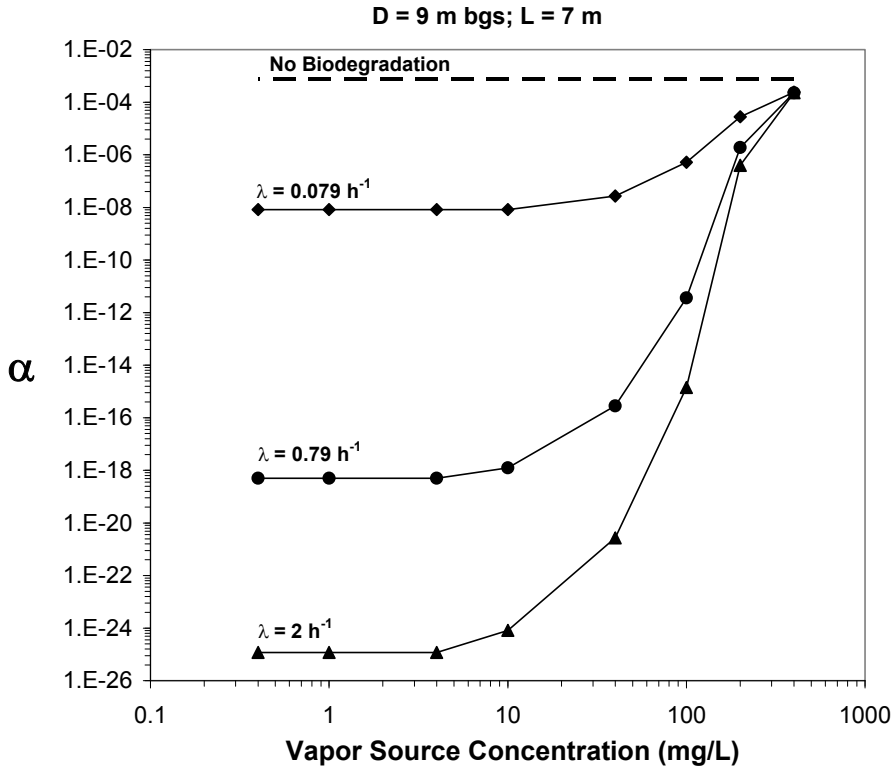

D = Source depth below ground surface
L = source foundation separation

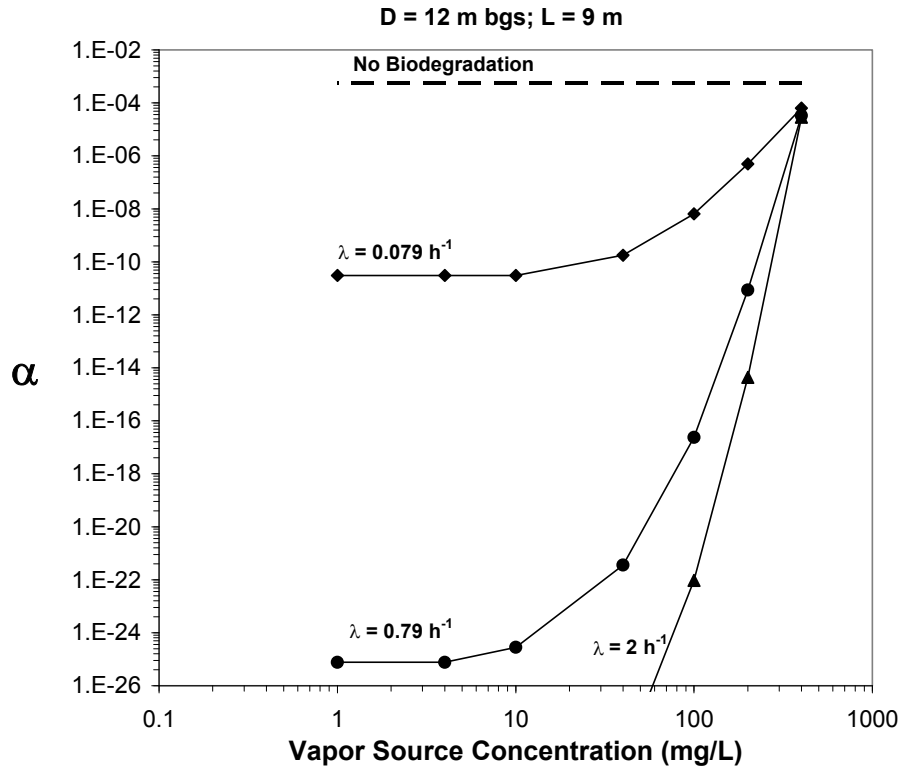

D = Source depth below ground surface
L = source foundation separation

Appendix C

Plots of Attenuation Factors as a Function of Source Concentration, Depth and First-order Biodegradation Rates for Slab-on-grade Scenarios

Introduction

This appendix summarizes the attenuation factors predicted in this work for slab-on-grade scenarios on homogeneous sandy soils, building constant under-pressurization of 5 Pa and full-perimeter cracks. The α-values are presented as a function of source-foundation separation for a vapor source concentration of 10 mg/L (this graph is application to all vapor source concentrations that smaller than 10 mg/L) and α-values are presented as a function of vapor source concentration for several source depths (D) and equivalent source-foundation separation (L). All graphs present α-values for three biodegradation rates (λ) and for the no-biodegradation case for comparison purposes.

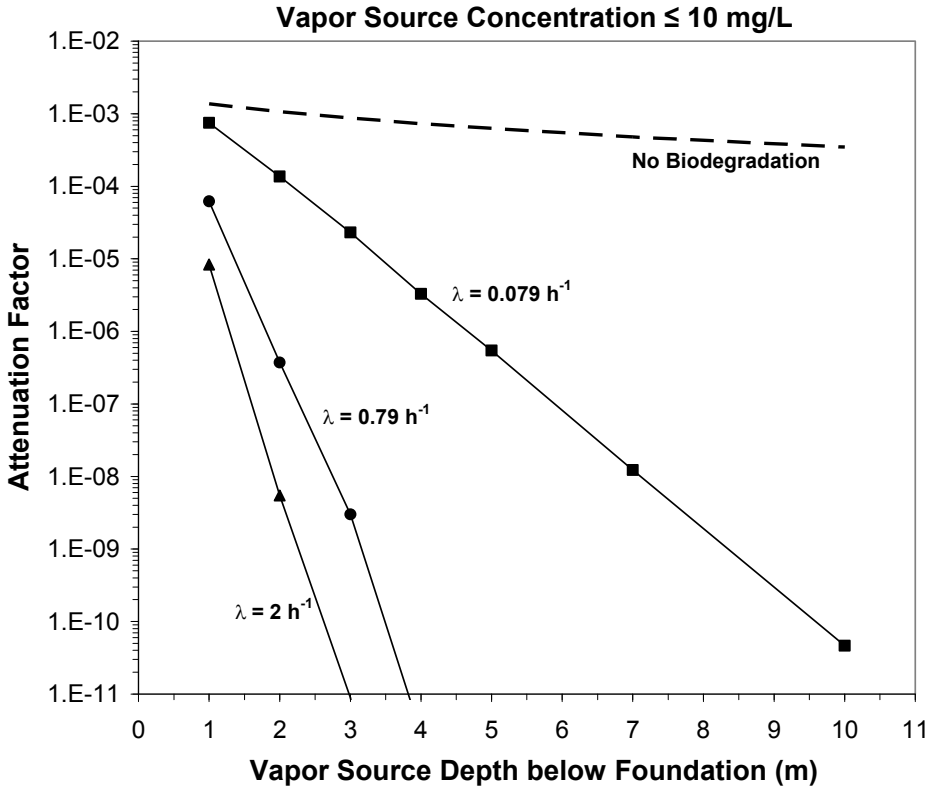

D = Source depth below ground surface
L = source foundation separation

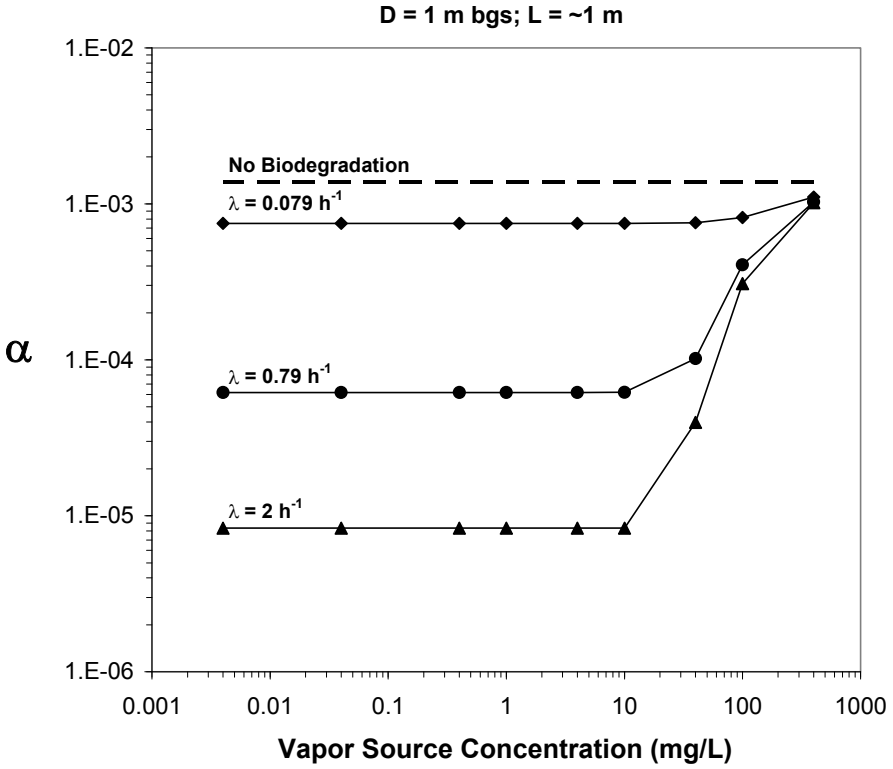

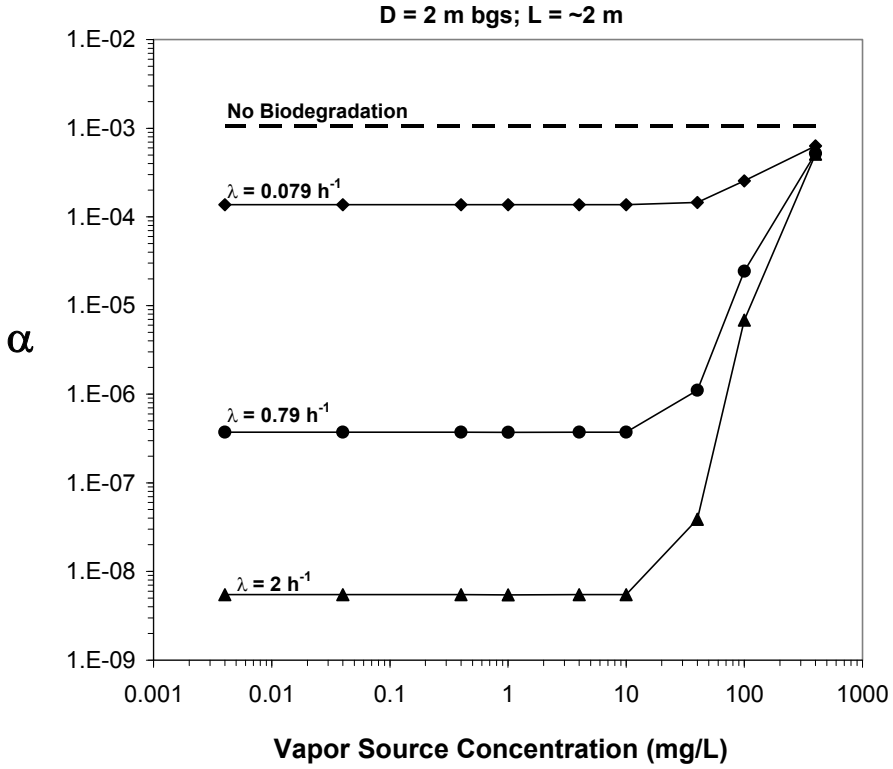

D = Source depth below ground surface
L = source foundation separation

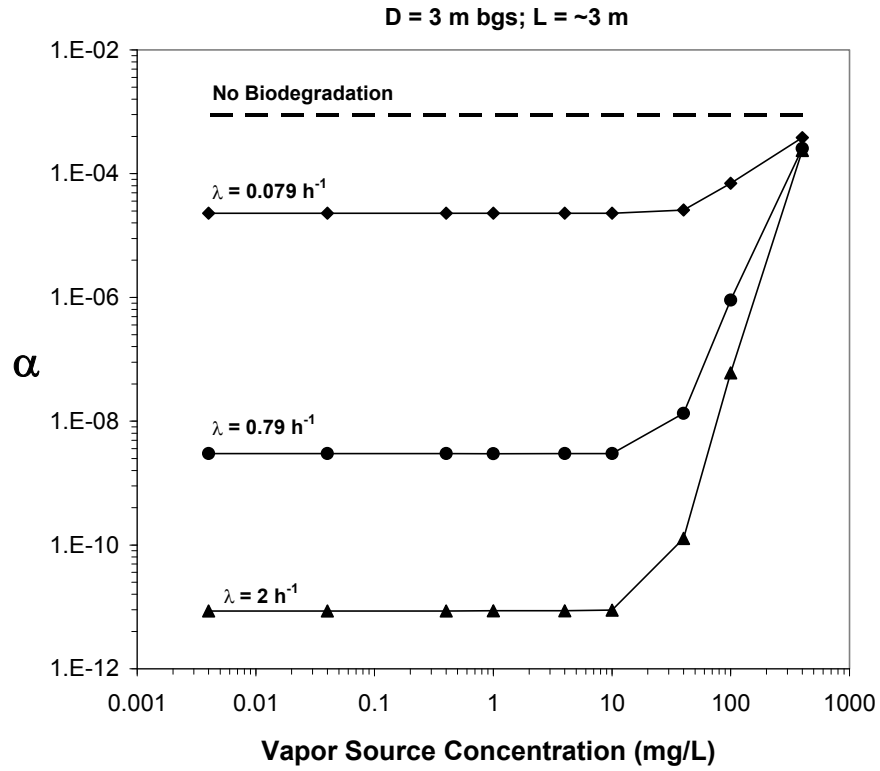

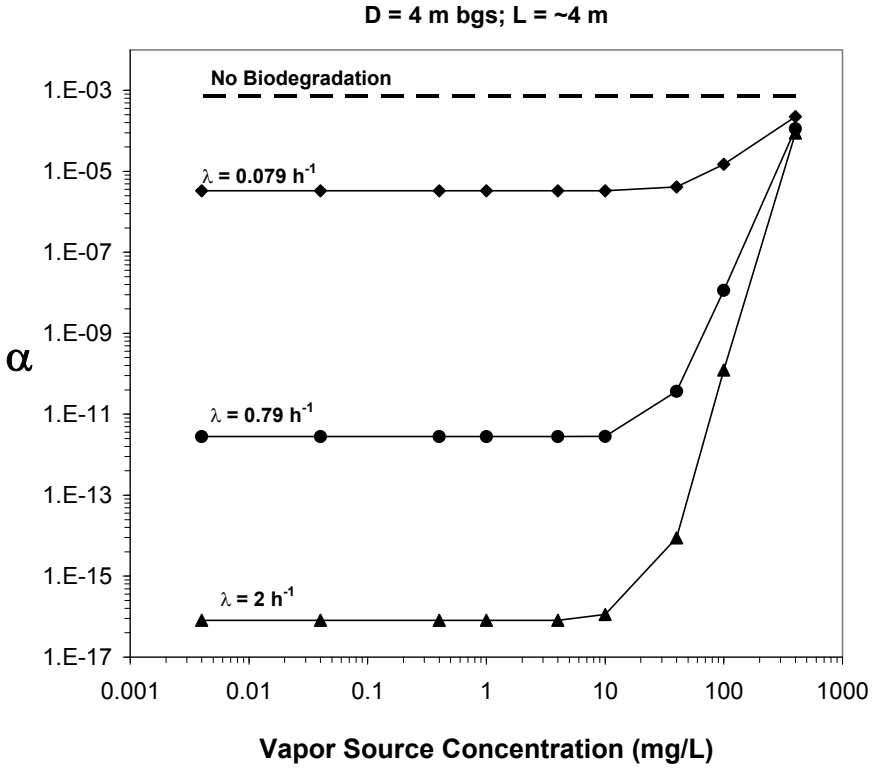

D = Source depth below ground surface
L = source foundation separation

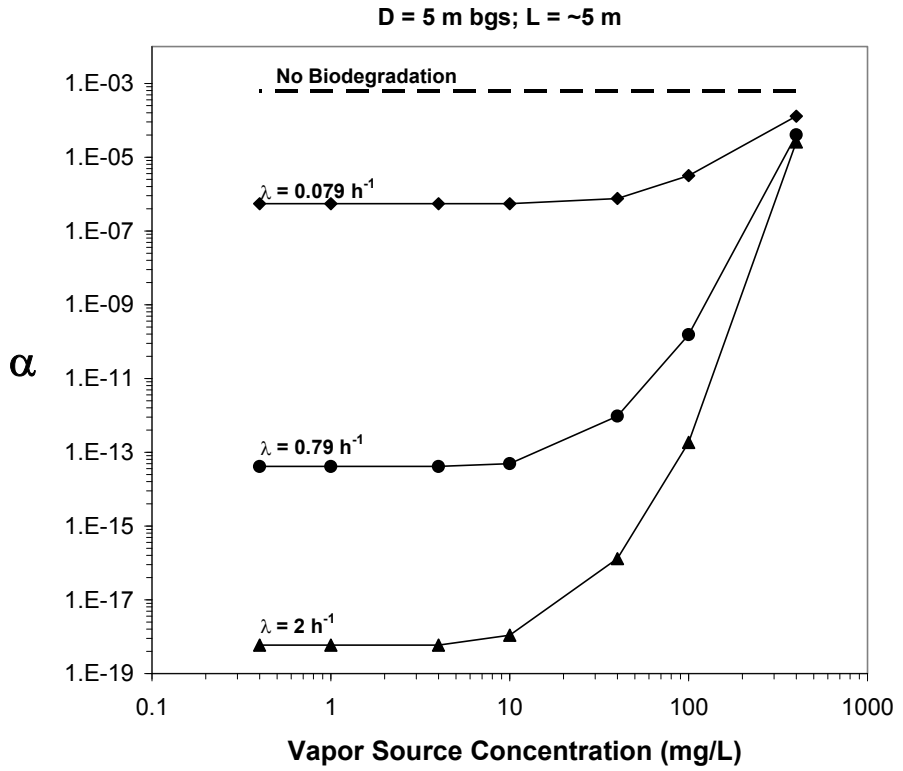

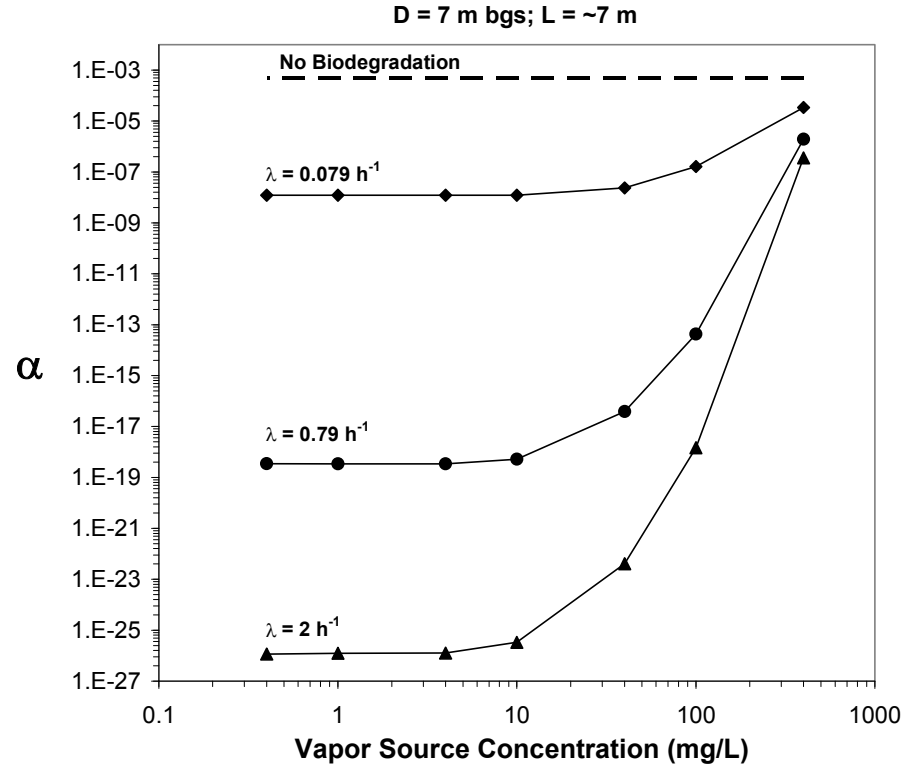

D = Source depth below ground surface
L = source foundation separation

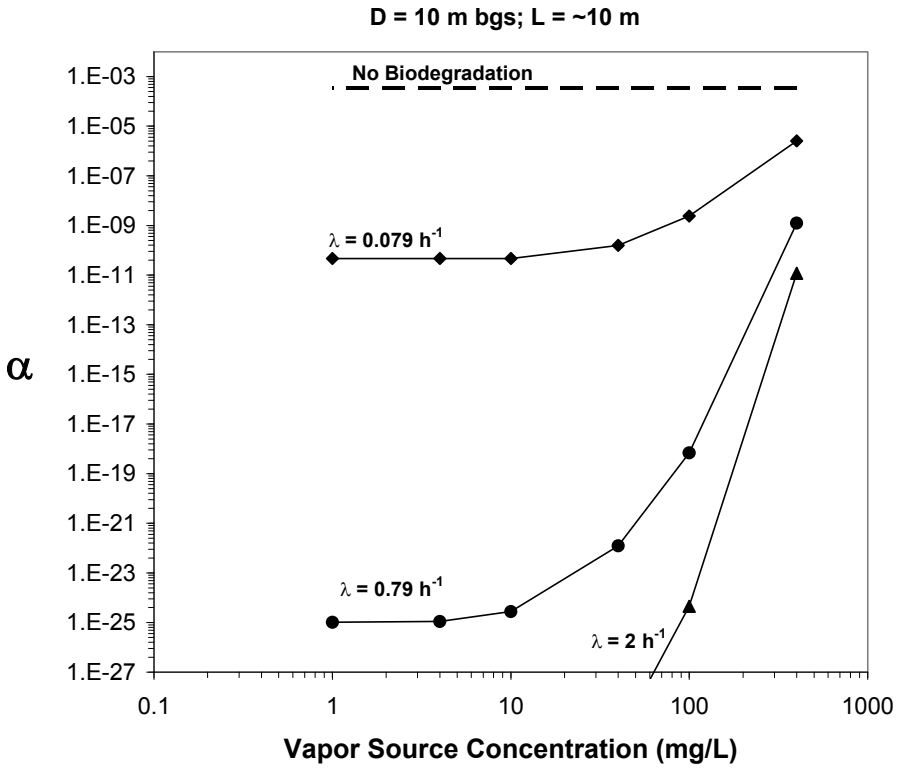

D = Source depth below ground surface
L = source foundation separation

1220 L Street, NW
Washington, DC 20005-4070
USA

202.682.8000

Additional copies are available through IHS
Phone Orders: 1-800-854-7179 (Toll-free in the U.S. and Canada)
303-397-7956 (Local and International)
Fax Orders: 303-397-2740
Online Orders: global.ihs.com

Information about API Publications, Programs and Services
is available on the web at www.api.org

Product No. I47750